



Optical Stochastic Cooling Experiment at the Fermilab IOTA ring

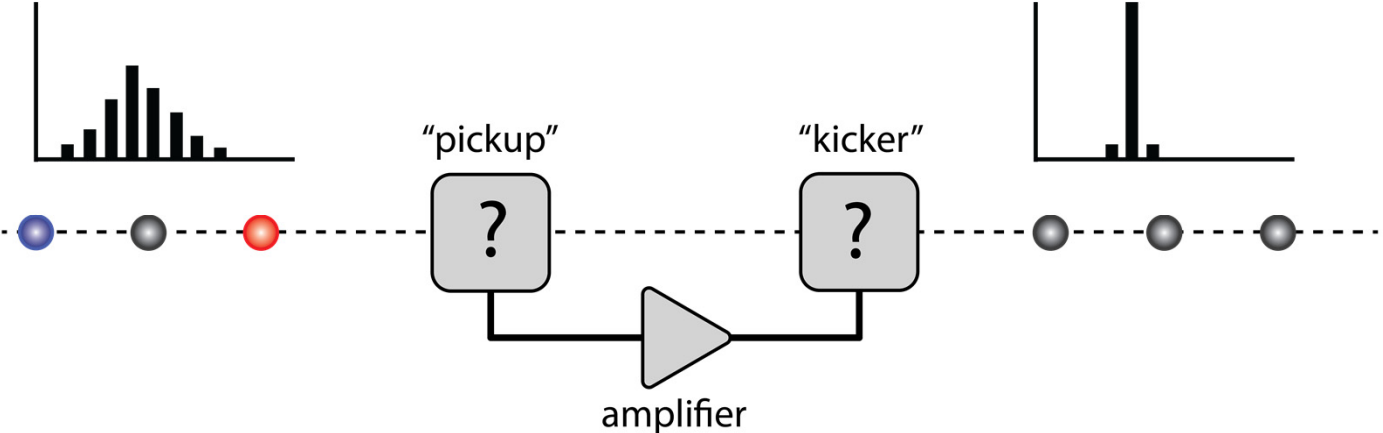
Jonathan Jarvis (FNAL)

ICFA Workshop on High-Intensity and High-Brightness Hadron Beams

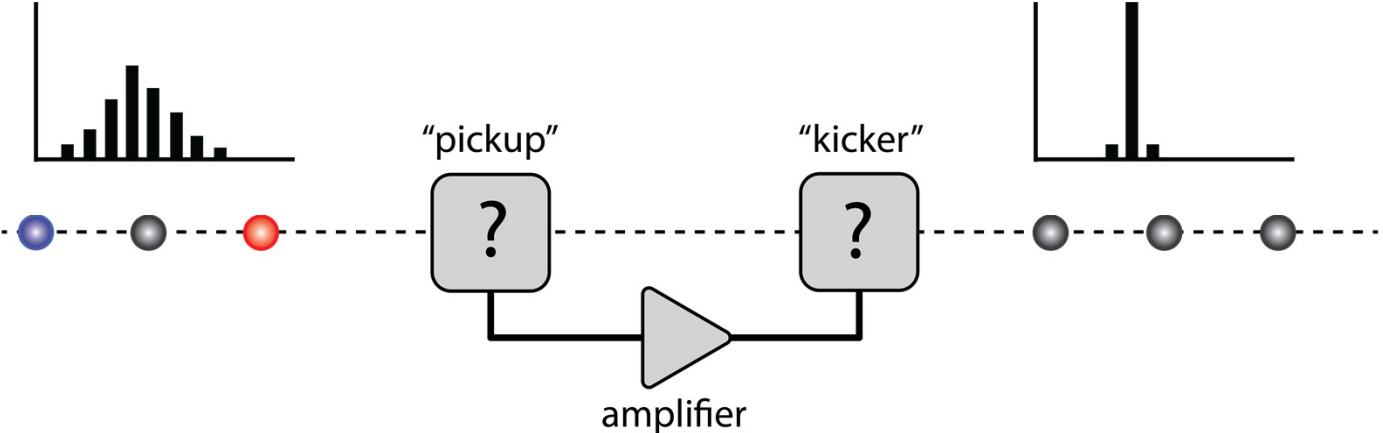
June 18-22, 2018

Daejeon, Korea

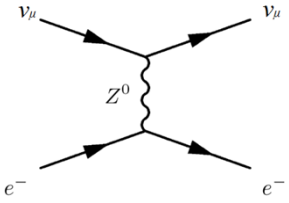
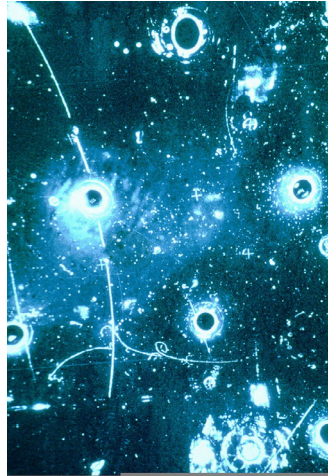
Stochastic Cooling: “van der Meer’s demon”



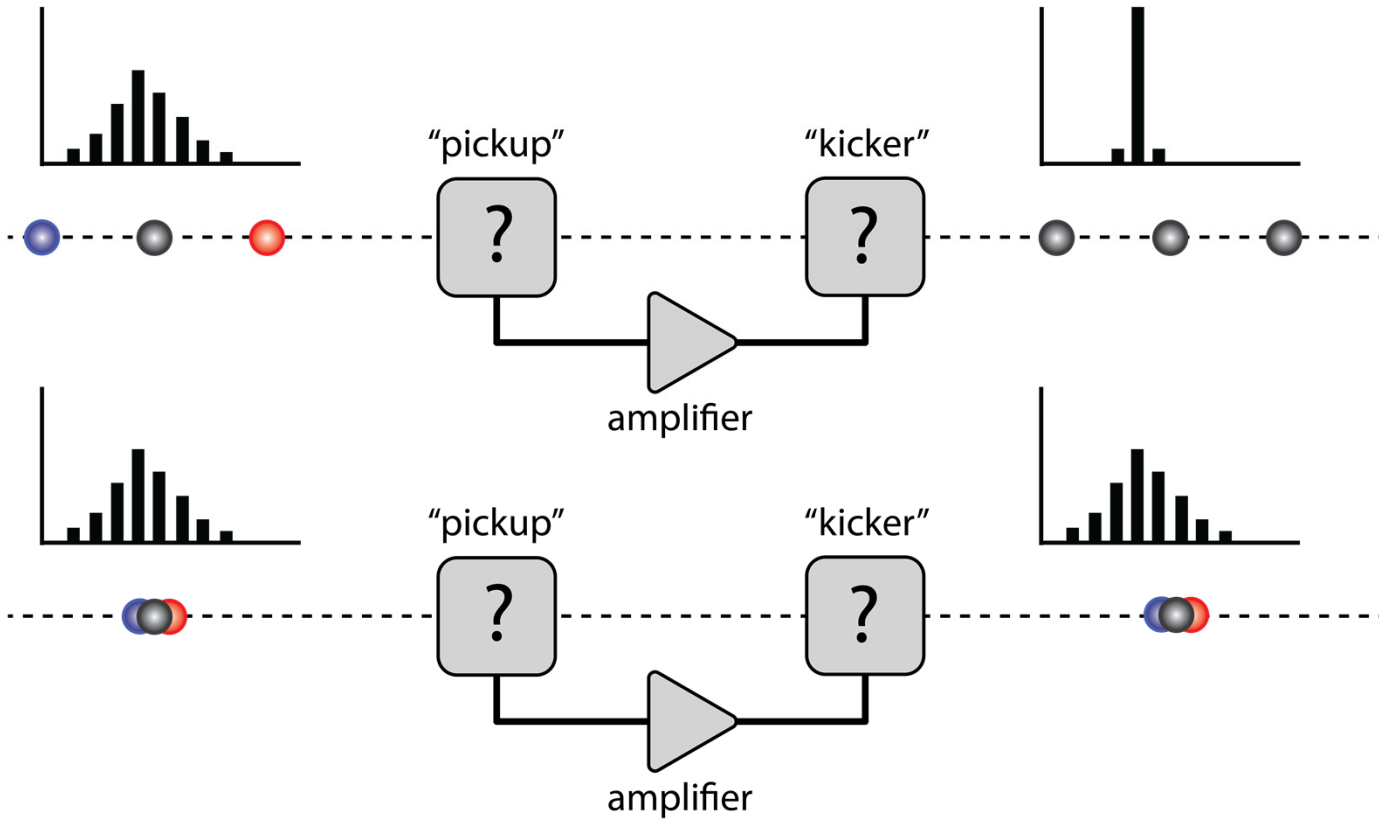
Stochastic Cooling: “van der Meer’s demon”



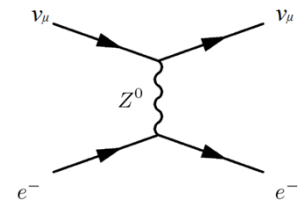
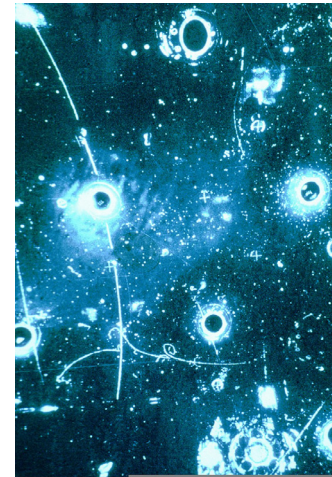
$$\mathcal{L} \sim \frac{f N_b N^2}{4\pi \sigma_x \sigma_y}$$



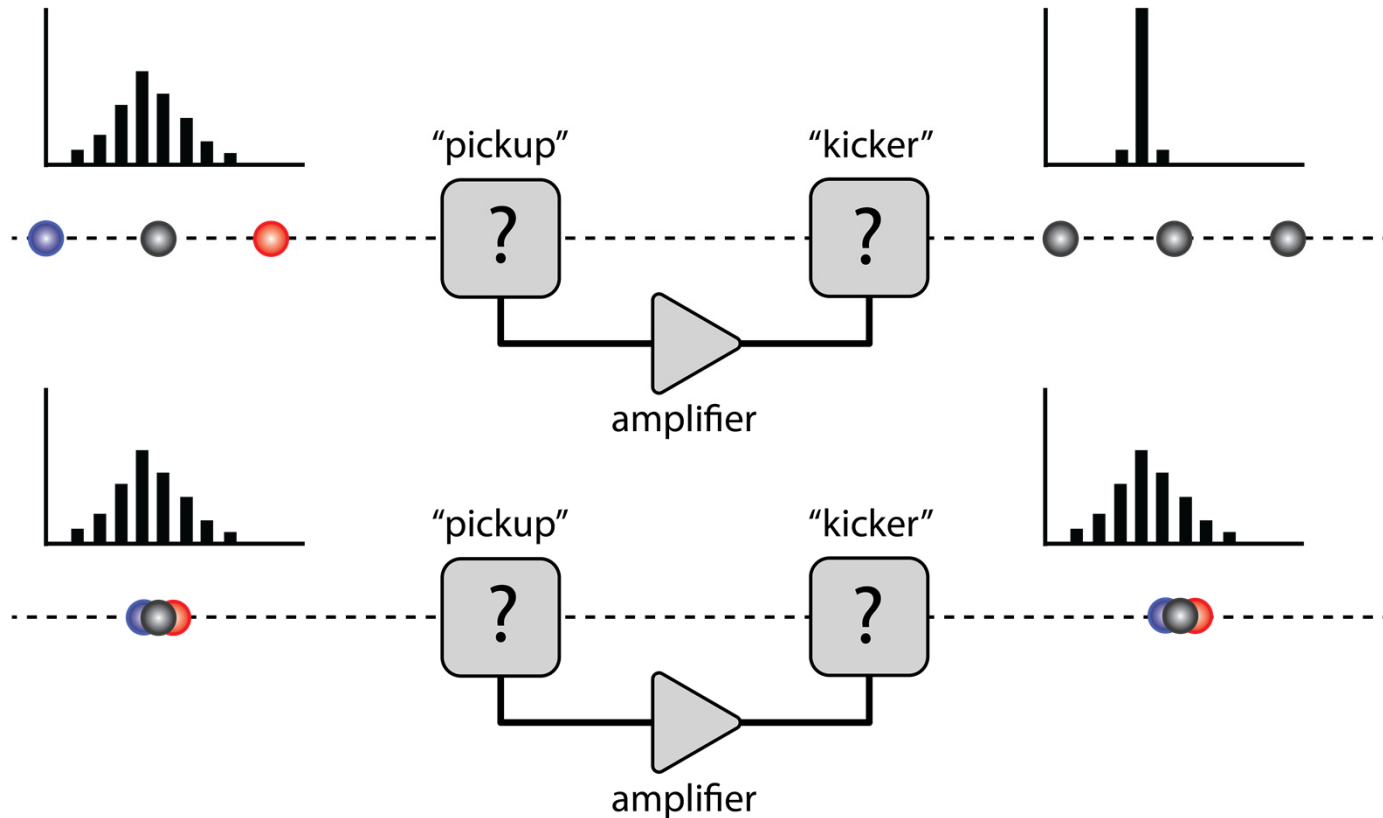
Stochastic Cooling: “van der Meer’s demon”



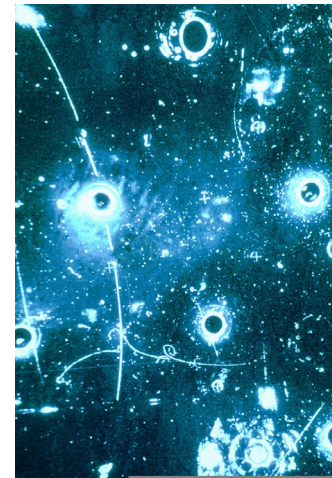
$$\mathcal{L} \sim \frac{f N_b N^2}{4\pi\sigma_x \sigma_y}$$



Stochastic Cooling: “van der Meer’s demon”

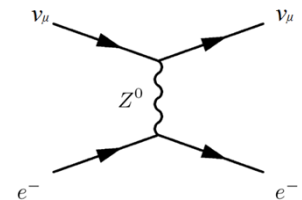


$$\mathcal{L} \sim \frac{f N_b N^2}{4\pi\sigma_x^* \sigma_y^*}$$

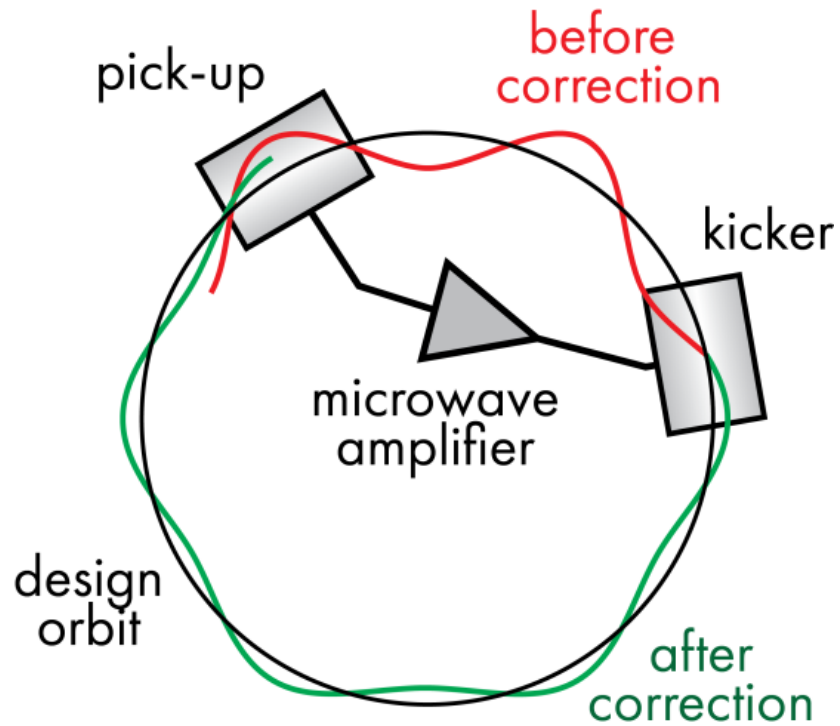


1) We can beat Liouville’s theorem (local phase-space density const.) if we have granular information about the beam ensemble.

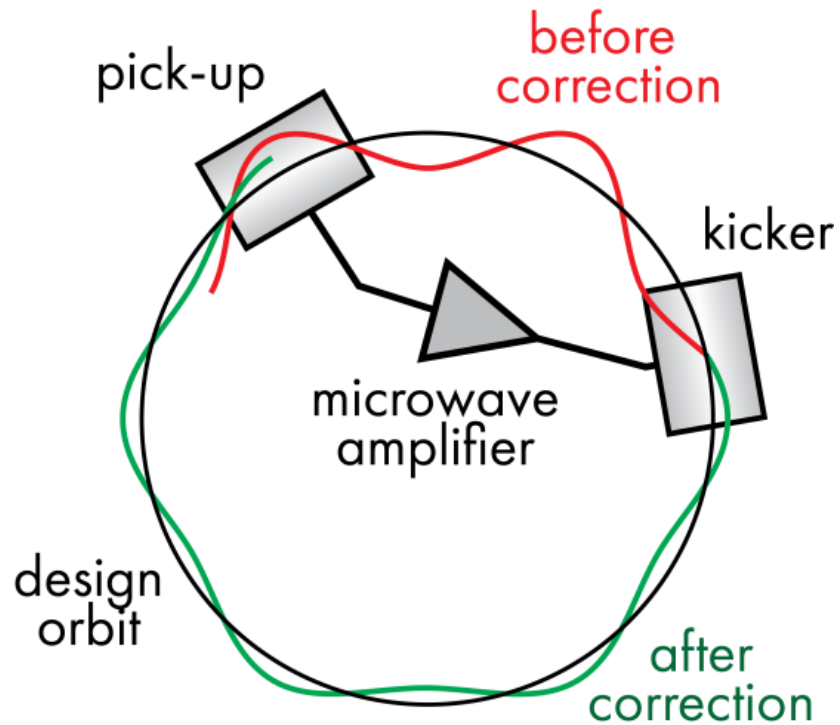
2) Bandwidth of feedback system controls cooling rate



Up to now, SC limited to ~GHz bandwidth



Up to now, SC limited to ~GHz bandwidth



- SC is a competition between coherent cooling effect of a particle's own signal and the incoherent heating effect of all other particles within a response time.
- Increase BW to enhance the relative strength of coherent component

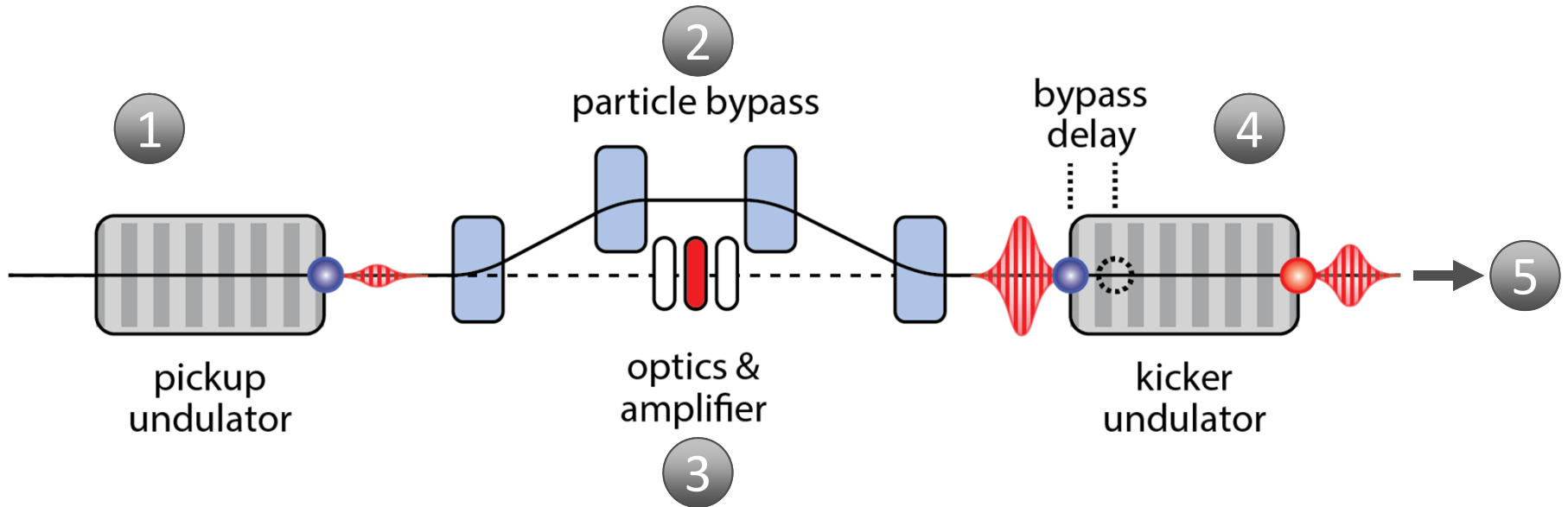
$$\frac{1}{\tau} = \frac{2W}{N} (2g - g^2)$$

↑ cooling ↑ heating

g : fraction of total sample error corrected per pass
 N : total # of particles in ensemble
 W : bandwidth of feedback system (Hz)
 τ : cooling time for beam variance (seconds)

(Assumptions!)

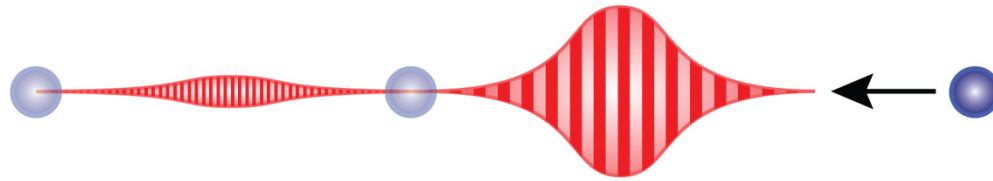
OSC extends the SC principle to optical bandwidth

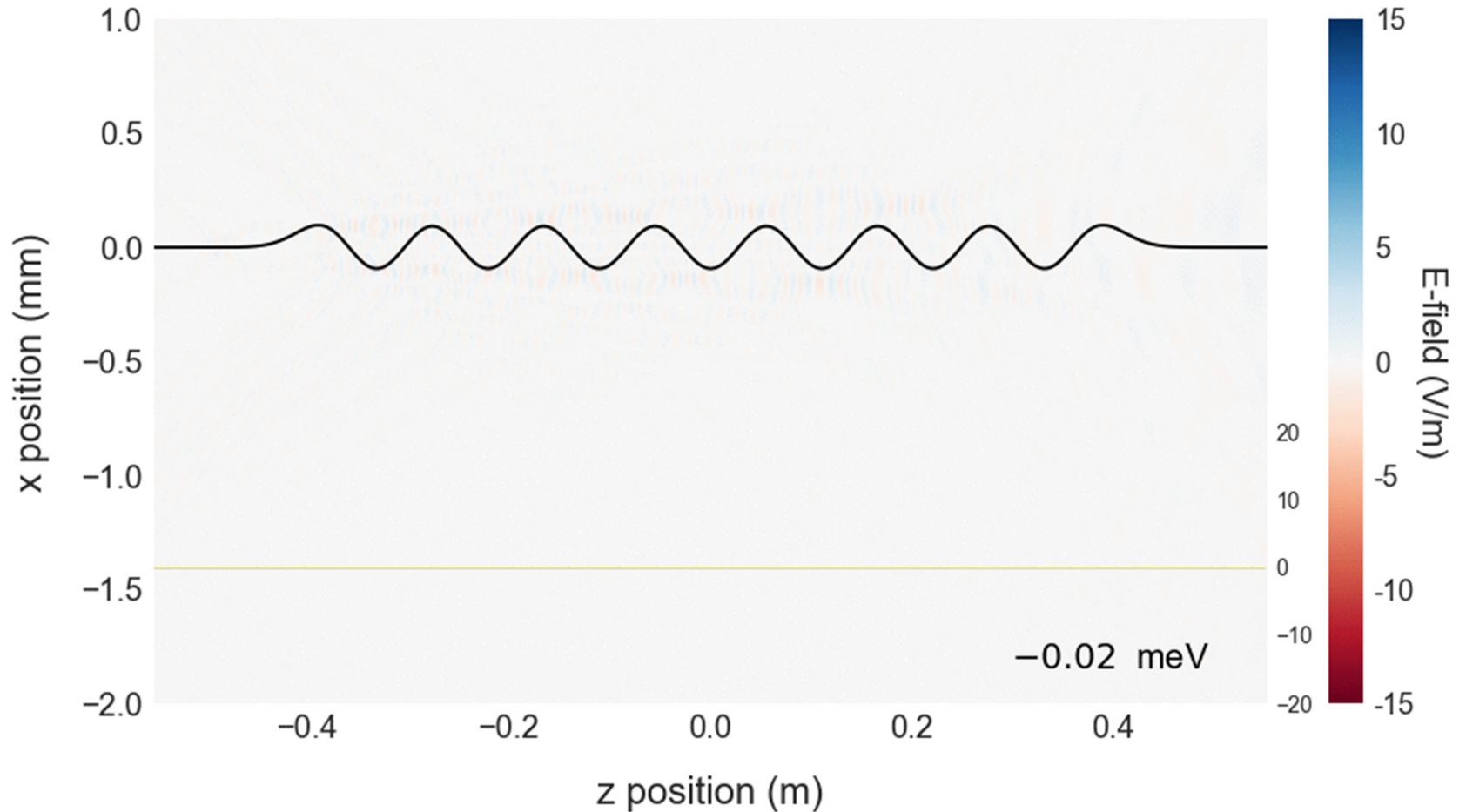
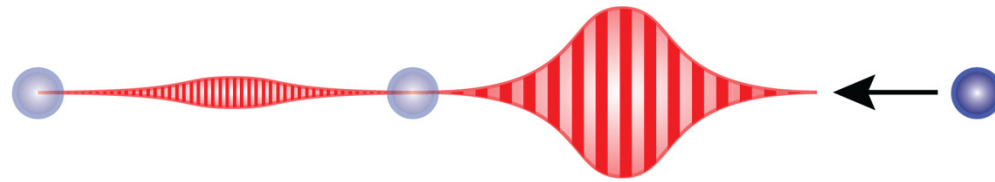


1. Each particle generates EM wavepacket in pickup undulator
2. Particle's properties are "encoded" by transit through a bypass
3. EM wavepacket is amplified (or not) and focused into kicker und.
4. Induced delay relative to wavepacket results in corrective kick
5. Coherent contribution (cooling) accumulates over many turns

[1] A.A.Mikhailichenko, M.S. Zolotarev, "Optical stochastic cooling," Phys. Rev. Lett. 71 (25), p. 4146 (1993)

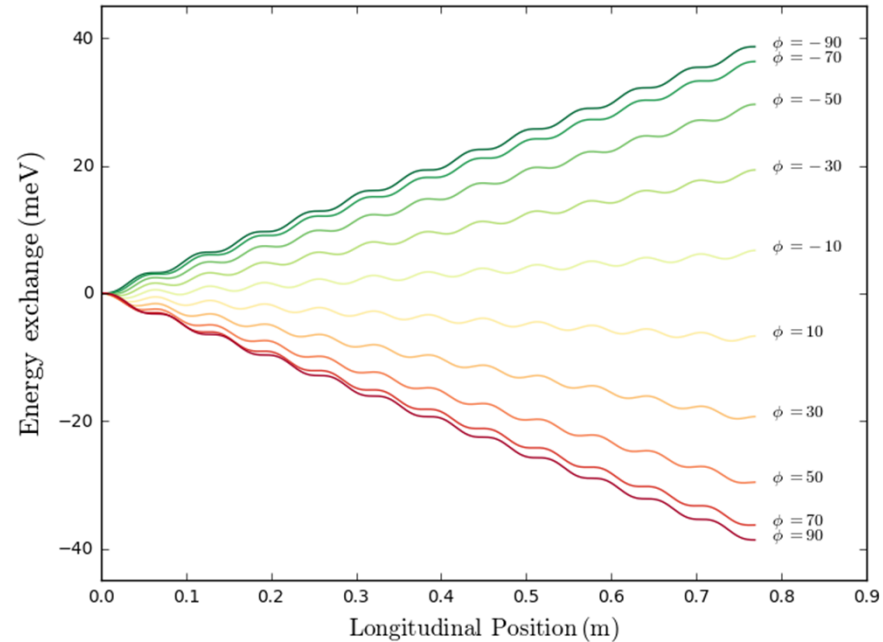
[2] M. S. Zolotarev, A. A. Zholents, "Transit-time method of optical stochastic cooling," Phys. Rev. E 50 (4), p. 3087 (1994)





Cooling force determined by mapping between undulators

- Reference particle experiences zero net energy change
- Max possible kick is twice the energy lost from emission in a single undulator
- For small deviations, cooling force is linear; nonlinear for large deviations
- Cooling force can reverse sign and cause heating/antidamping



$$\frac{\delta p}{p} = -\kappa \sin(k_0 s) = -\frac{\sqrt{G} \Delta E}{cp} \sin(k_0 s)$$

Most critical OSC parameters: cooling rates and ranges

rate : how fast

- In the linear approximation, path lengthening is:

$$s \approx (M_{51}D + M_{52}D' + M_{56}) \frac{\Delta p}{p} = S_{pk} \frac{\Delta p}{p}$$

- Can estimate cooling rate (sec^{-1}) for longitudinal emittance as:
- So for a given setting of the chicane (M_{56}) the cooling ratio is determined by the dispersion and its derivative at the exit of the pickup.
- We can then couple the horizontal and vertical DOF elsewhere in the ring to achieve full 6D cooling.

$$\lambda_s = f_0 \kappa k_0 S_{pk}$$

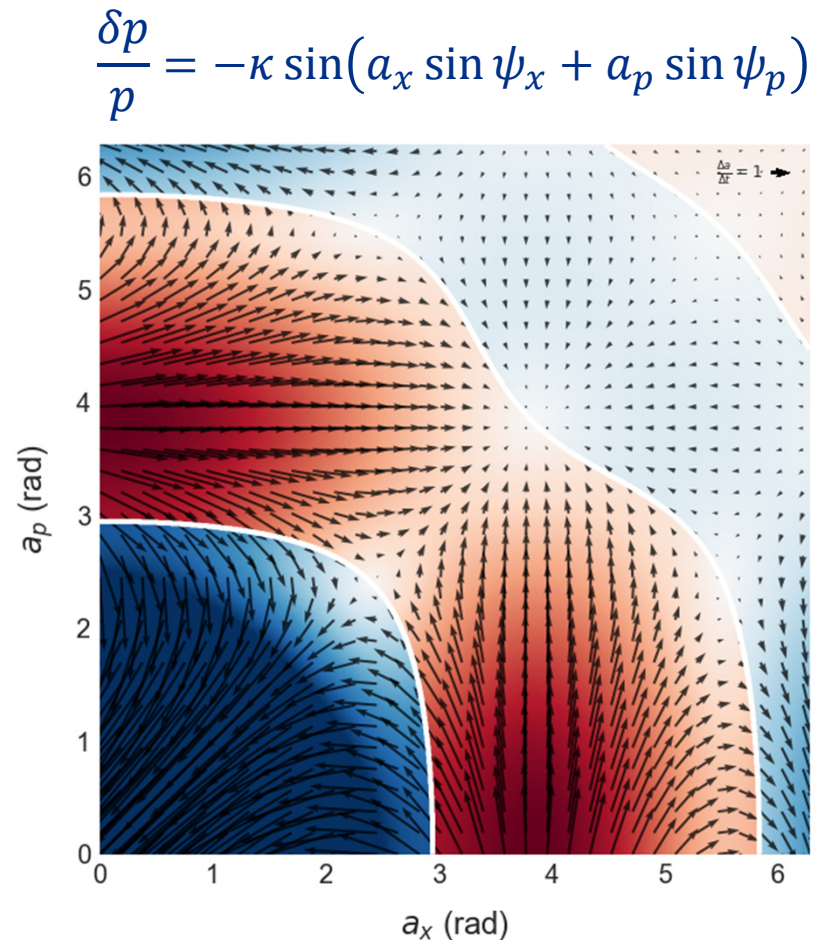
$$\frac{\lambda_x}{\lambda_s} = \frac{M_{56}}{S_{pk}} - 1$$

OSC creates a cooling/heating surface in phase space

range : how far

- On successive passes through the cooling insertion, particles will have different betatron and synchrotron coordinates
- Path lengthening depends on these coordinates, and the cooling force on a given pass increases or decreases
- Integrating over betatron and synchrotron periods reveals the cooling range for OSC ($\mu_{01} = 2.405$)
- Optimum changes as beam is cooled

$$n_{\sigma x} = \sqrt{\frac{\epsilon_{max}}{\epsilon}} \quad n_{\sigma p} = \frac{\left(\frac{\Delta p}{p}\right)_{max}}{\sigma_p}$$



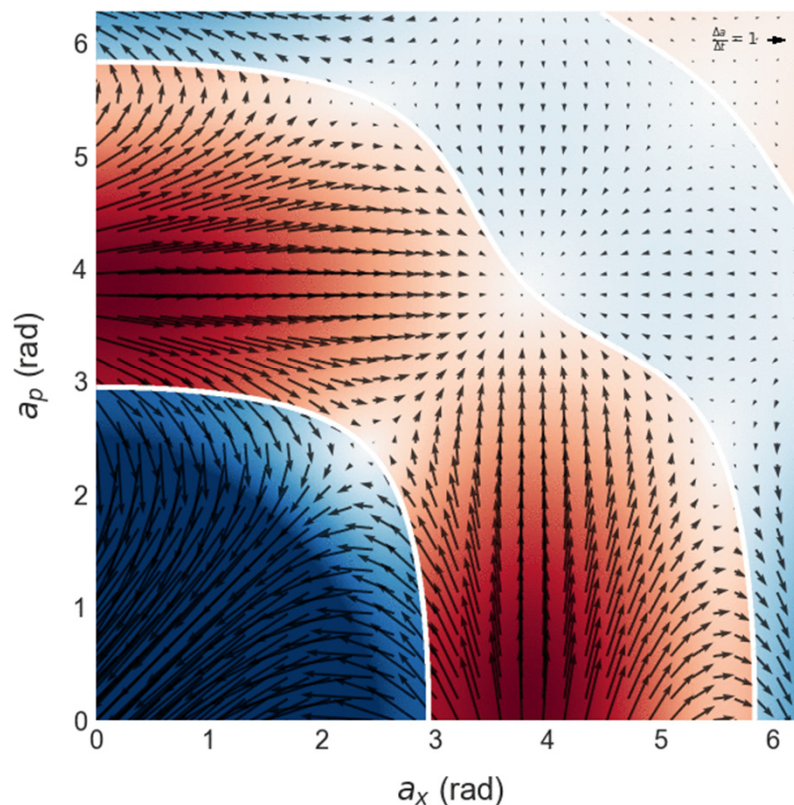
V. Lebedev, "OPTICAL STOCHASTIC COOLING" in Beam Dynamics Newsletter, No. 65

OSC creates a cooling/heating surface in phase space

range : how far

- On successive passes through the cooling insertion, particles will have different betatron and synchrotron coordinates
- Path lengthening depends on these coordinates, and the cooling force on a given pass increases or decreases
- Integrating over betatron and synchrotron periods reveals the cooling range for OSC ($\mu_{01} = 2.405$)
- Optimum changes as beam is cooled

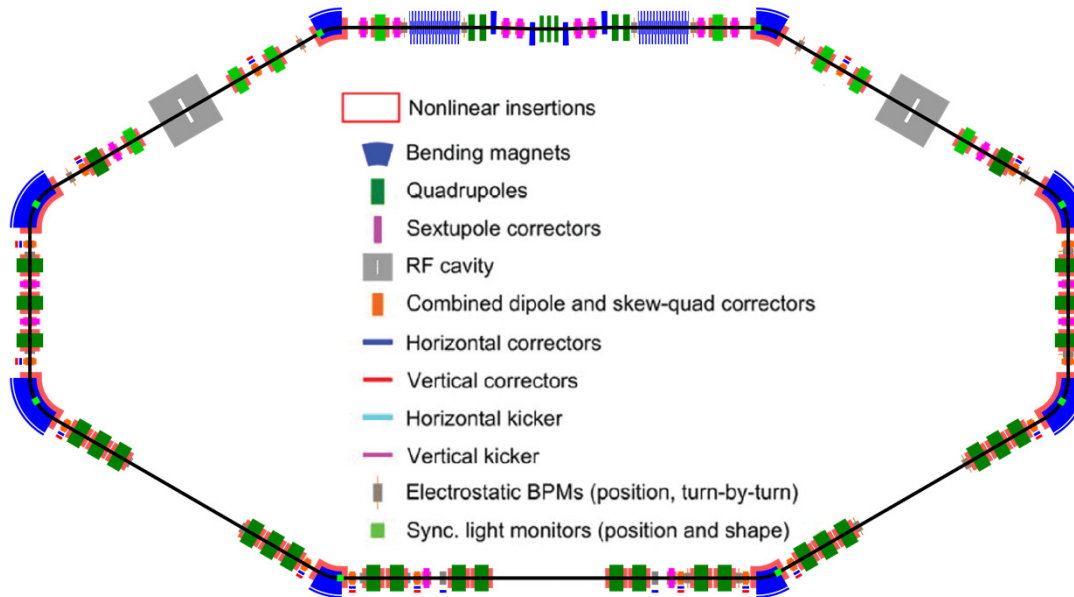
$$\frac{\delta p}{p} = -\kappa \sin(a_x \sin \psi_x + a_p \sin \psi_p)$$



$$n_{\sigma x} = \sqrt{\frac{\varepsilon_{max}}{\varepsilon}} \quad n_{\sigma p} = \frac{\left(\frac{\Delta p}{p}\right)_{max}}{\sigma_p}$$

V. Lebedev, "OPTICAL STOCHASTIC COOLING" in Beam Dynamics Newsletter, No. 65

IOTA: designed with OSC as a key requirement

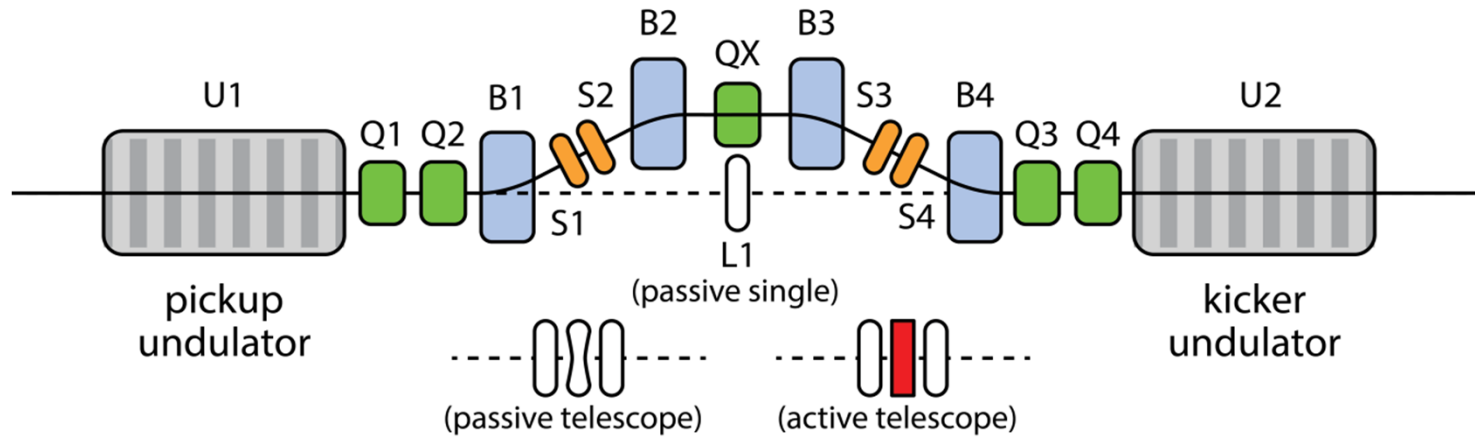


Beam kinetic energy	100 MeV
Rms momentum spread, σ_p	$1.06 \cdot 10^{-4}$
x-emittance (rms); S.Rad w/no OSC, ε	2.62 nm
Delay in the cooling chicane, Δs	2 mm
Offset in the chicane, h	35.1 mm
Ratio of OSC (no x-y coupling), λ_x / λ_s	1.16
Cooling ranges (no x-y coupling), $n_{\sigma x} / n_{\sigma s}$	10 / 4.4
Und. radiation wavelength, $2\pi/k_0$	2.2 μm
Beta-function in chicane center, β^*	0.12 m
Disp. in chicane center, D^*	0.48 m
Disp. invariant in chicane center, \mathcal{H}^*	1.92 m
Max. energy kick, ΔE	22 meV
OSC horiz. cooling rate (no x-y coupling)	20 s^{-1}
OSC long. cooling rate (no x-y coupling)	17 s^{-1}

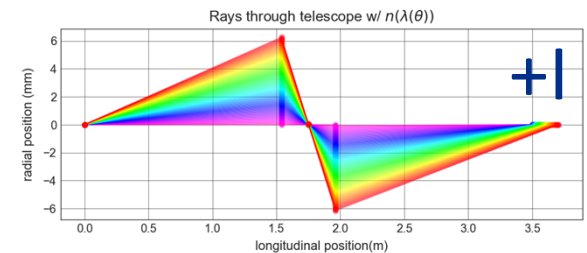
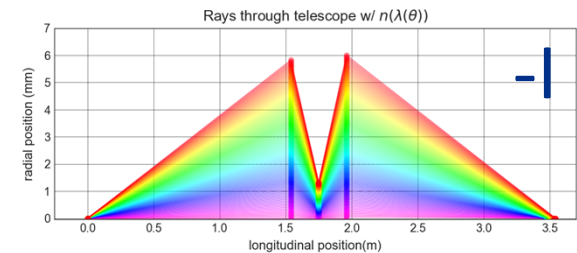
- Low energy (100 MeV) reduces equilibrium emittance, energy spread and increases synchrotron radiation damping time
- Improves cooling ranges and increases the relative strength of OSC
- IOTA's passive OSC can beat sync. rad by as much as 60x

For a detailed look at IOTA OSC lattice, orbit correction, magnets etc... recent FAST/IOTA workshop <https://indico.fnal.gov/event/16269/contribution/48> (A. Romanov)

The IOTA OSC concept and configurations

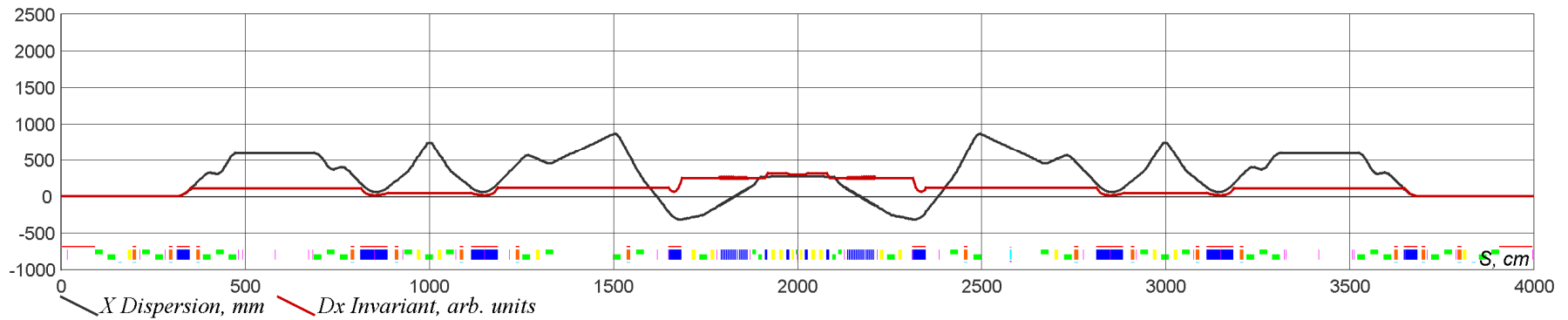
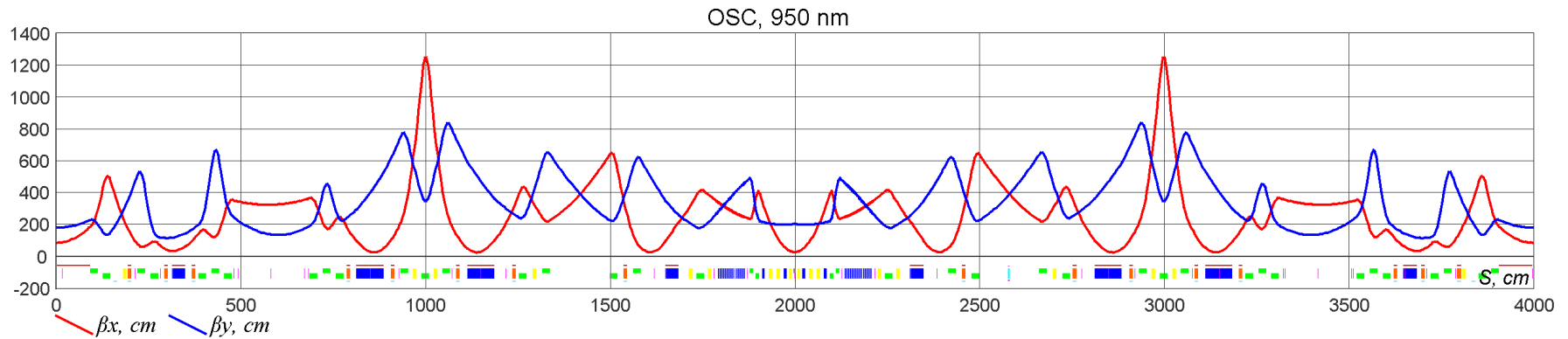


- Three configurations under development:
 - “1- μm ” passive
 - “2- μm ” passive & active
- Collider-style optics for optimum performance
- Coupling quad (QX) for controlling coupling of transverse and longitudinal cooling
- Sextupoles for reduction of non-linear path lengthening



Linear lattice design for 950 nm

A. Romanov

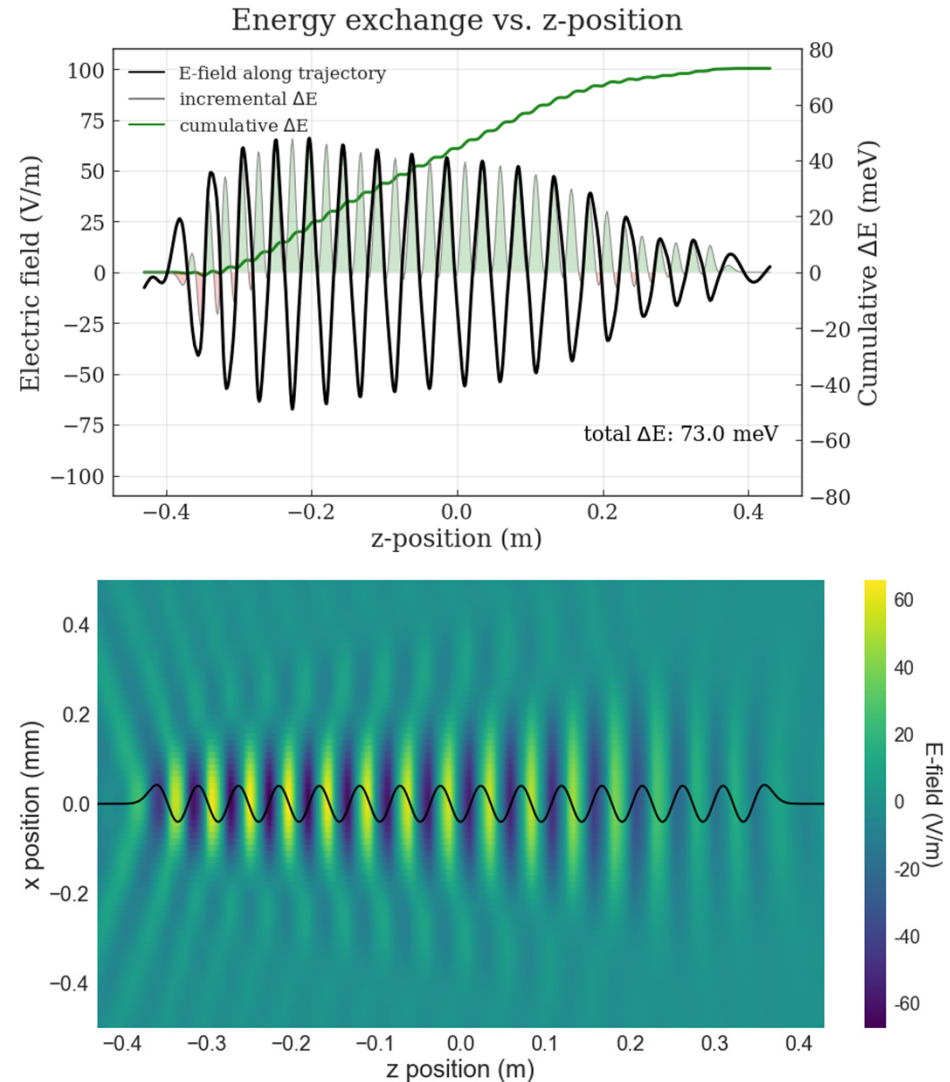


Betas start, x,y	25, 200 cm
D_x start	27 cm
Tunes, x,y	5.42, 2.42
Mom. comp.	0.0025
Emittances, x,y	0.5 E-7 cm

Energy drop	13.4 eV
Bunch length @30V	7.6 cm
Energy spread	1.00 E-4
Sync. Tune @30V	2.05 E-5
Damp. times (x,y,s)	(2.0,2.0,0.985) s

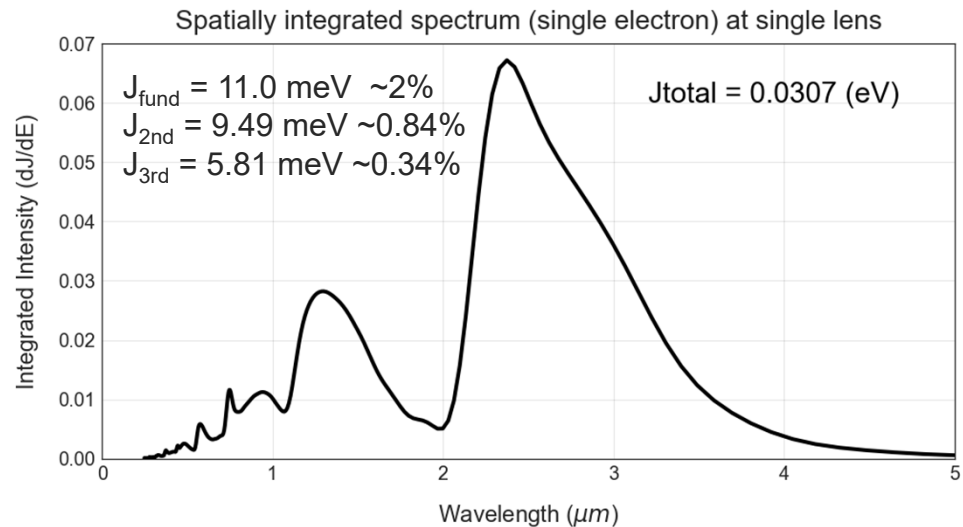
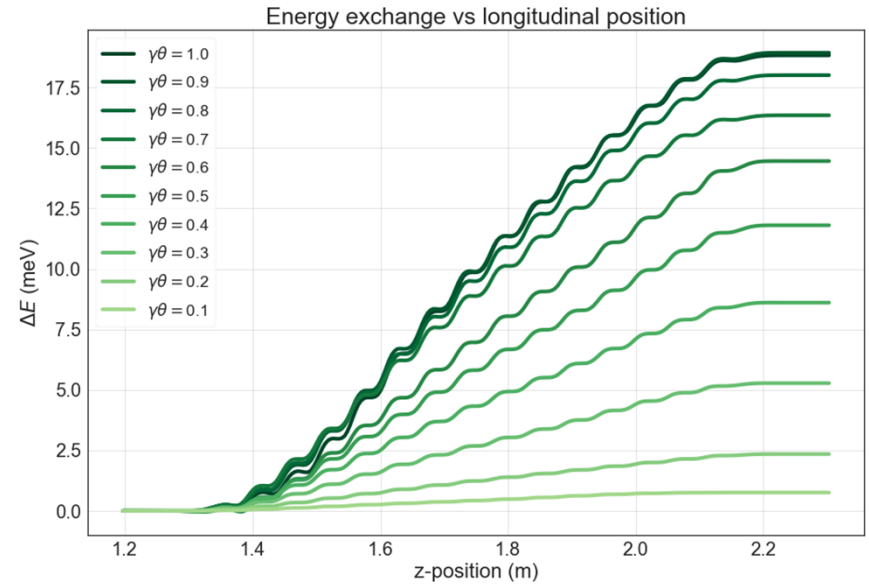
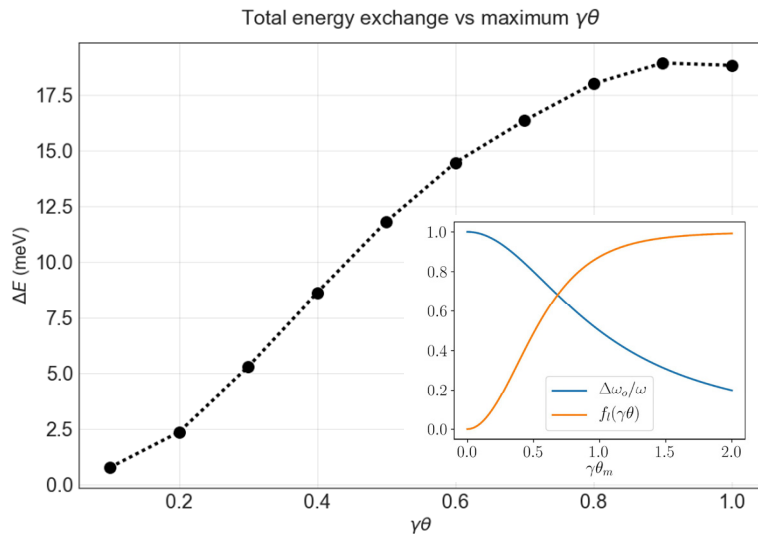
Performance of single lens makes 1-um (passive) possible

- A shorter wavelength requires reduced delay to maintain balance of rates and ranges
- Insufficient delay (<1mm) available for a telescopic optical system at $1\mu\text{m}$
- Single lens dramatically reduces complexity of optical system and associated risks
- Detectors in this range are far superior to those available at $2\mu\text{m}$; also improves compatibility with single-electron studies



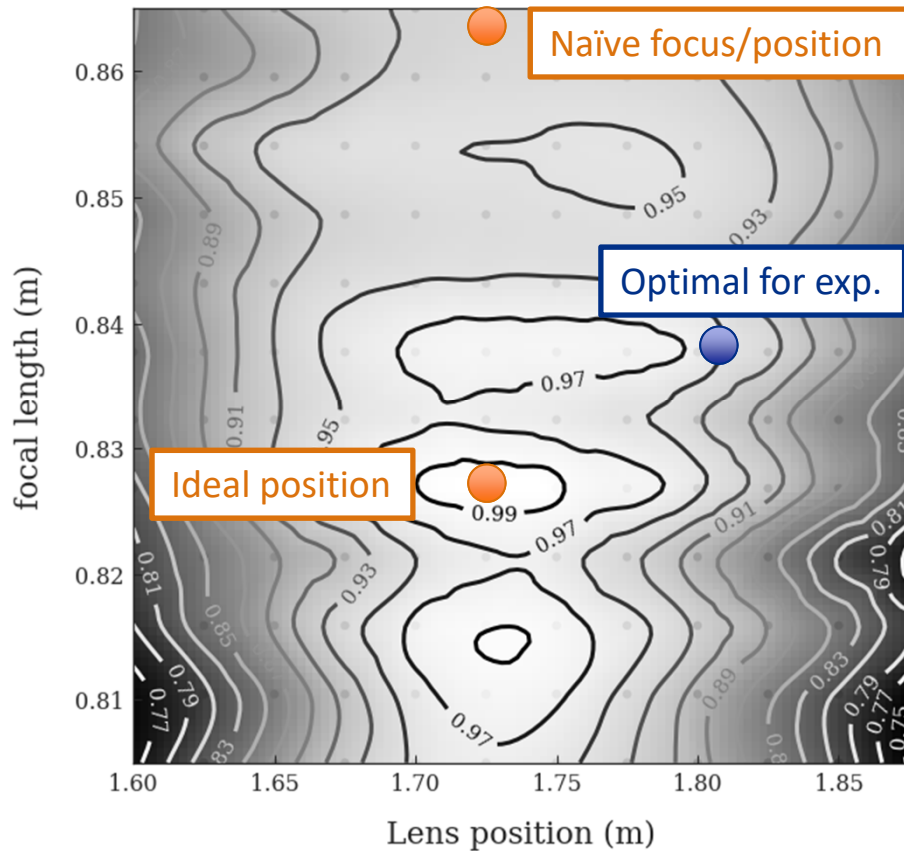
Maximum kick depends on collection angle

- Collection beyond $\gamma\theta = 0.8$ provides little benefit;
- For single lens, corresponds to ~ 7 -mm radius at center of OSC section
- Matches well with theory

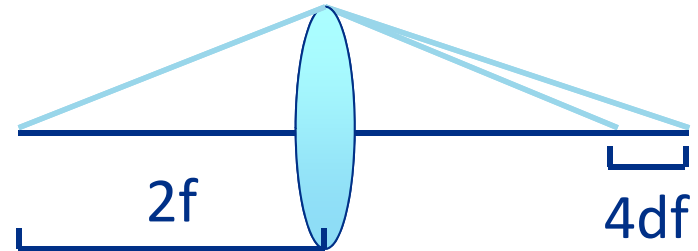
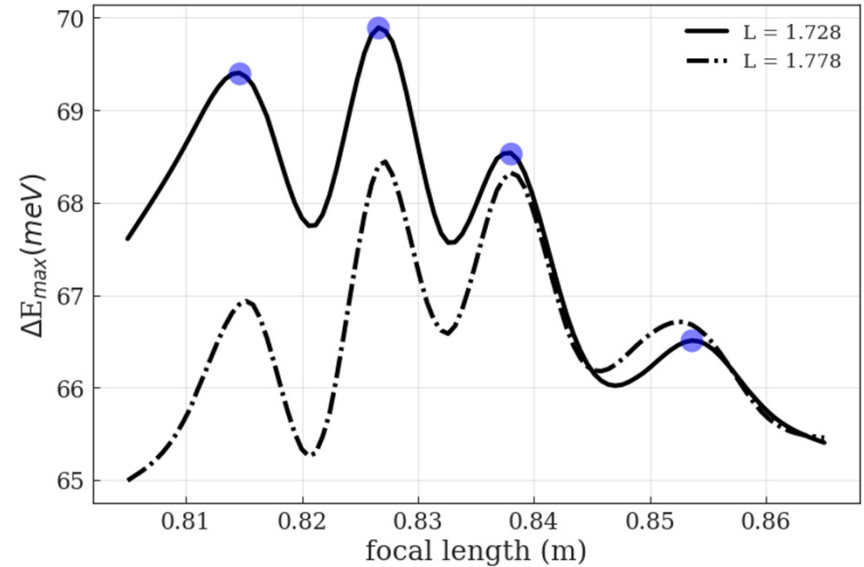


Optimize strength and position for max energy exchange

maximum ΔE vs (lens position, focal length)

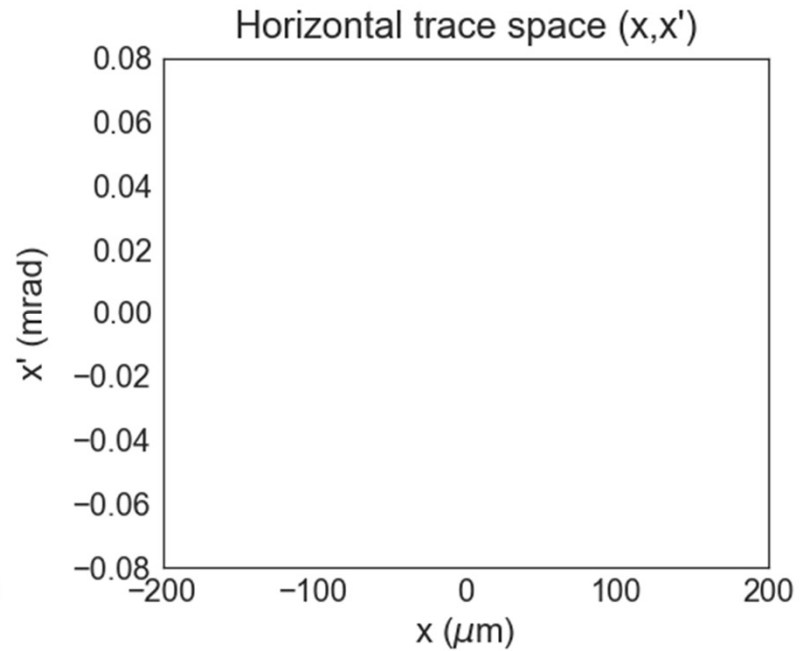
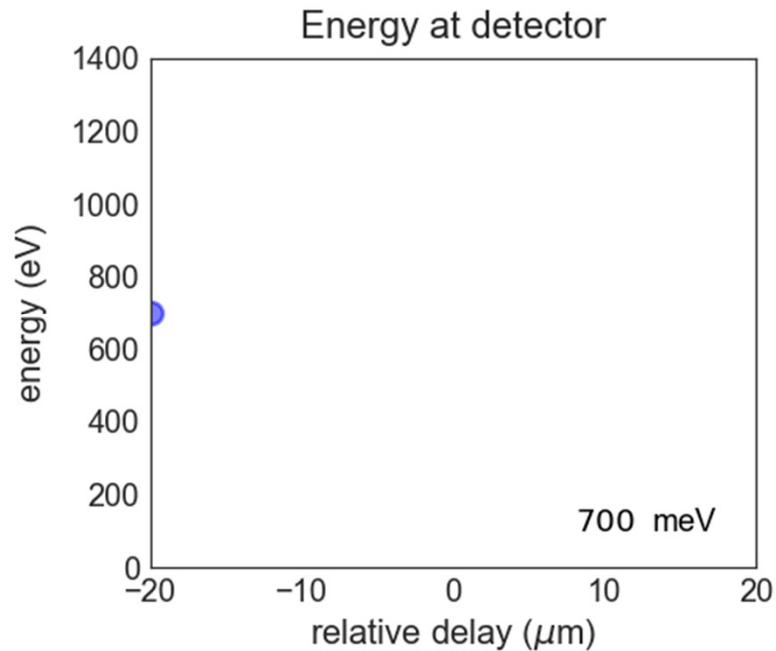


Effect of shifting lens by 50 mm



$$4df = 4.8\text{cm} \approx \lambda_u$$

Oscillation in radiation power when longitudinally aligned



- Total energy lost by single particle in both undulators is:
- Radiation from particles will add incoherently, but there will be a modulation of total power when bypass is near proper tuning

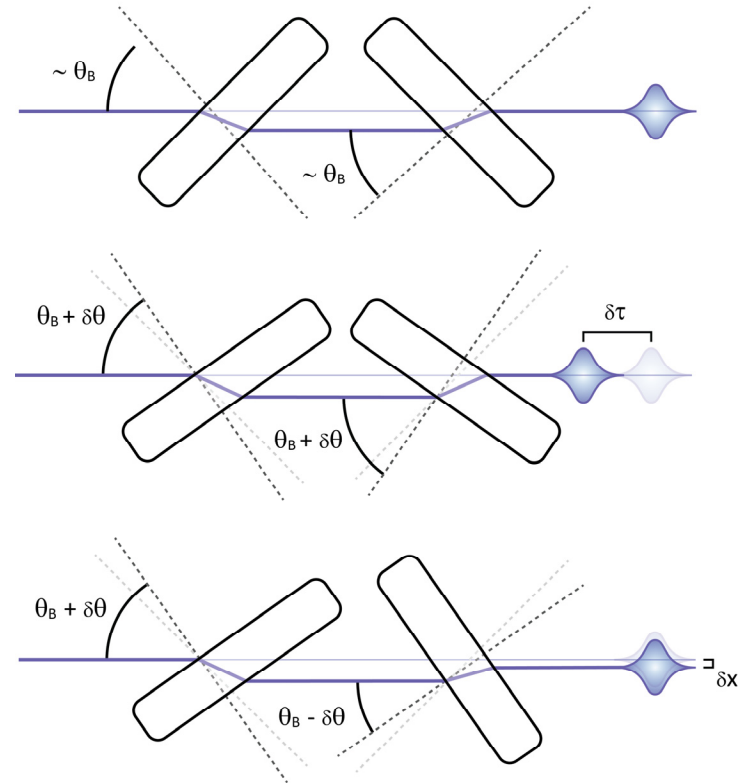
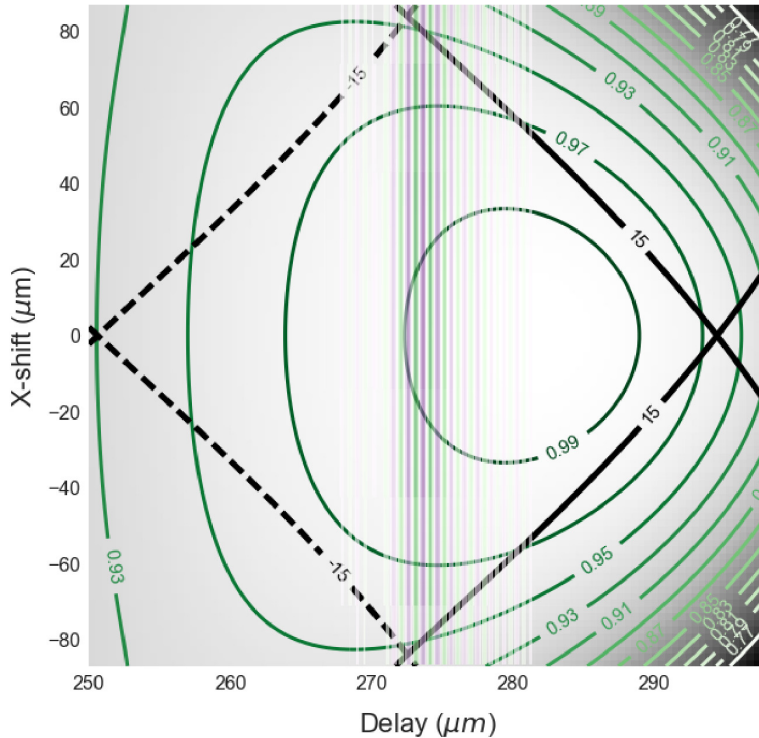
$$\Delta E(s) = -\Delta E_{tot} (1 + \sqrt{G} f_L (\gamma \theta_m) \sin(k_0 s))$$

- e.g. 1- μm , w/ InGaAs diode, signal to noise of $\sim 100\times$, for 10^3 electrons with 1-ms integration

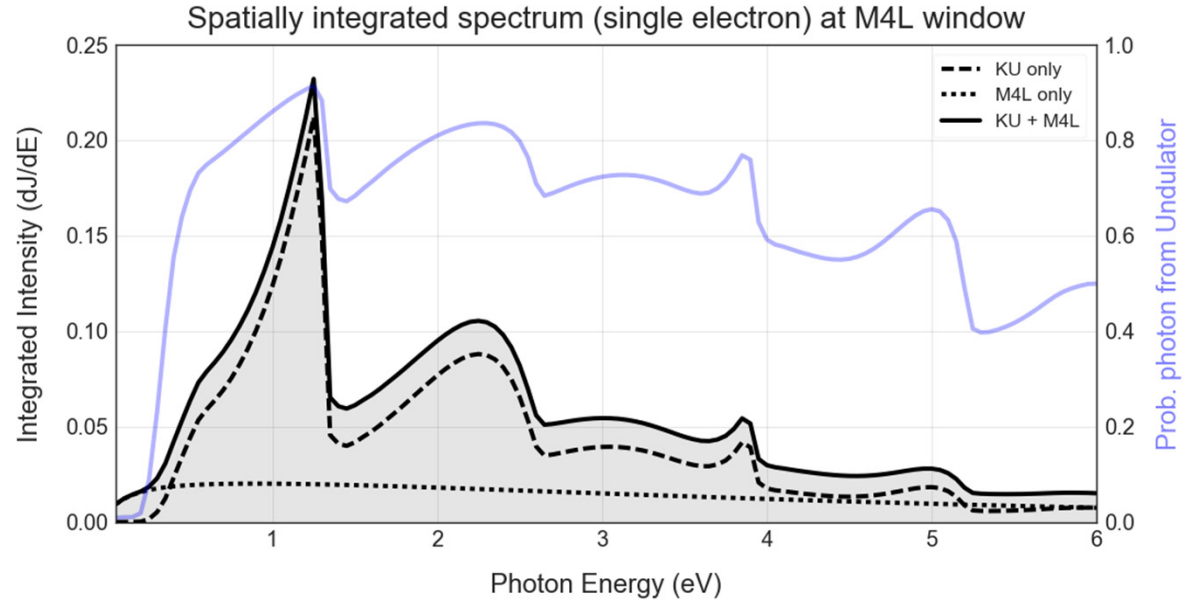
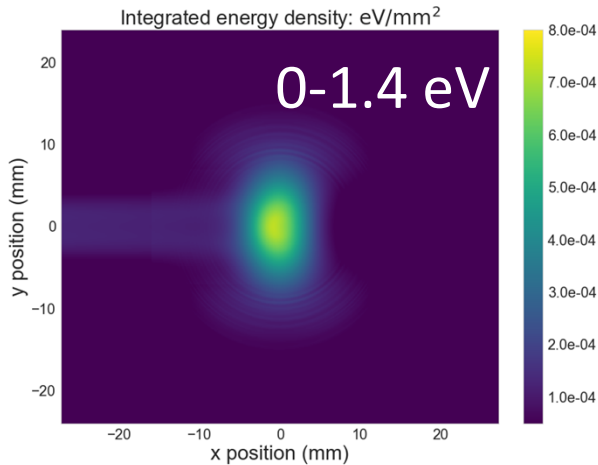
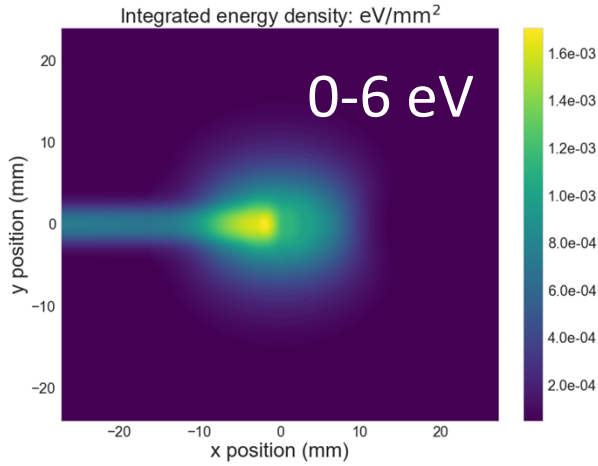
Fine tune alignment and delay with a single stage:

- Precision slabs centered near the Brewster angle
- Coordinated adjustment lets us independently select any longitudinal delay and transverse shift

Transmittance vs $(\Delta s, \Delta x)$: $t=250\text{-}\mu\text{m}$, $\lambda = 0.95\mu\text{m}$; $\theta_B = 7^\circ$

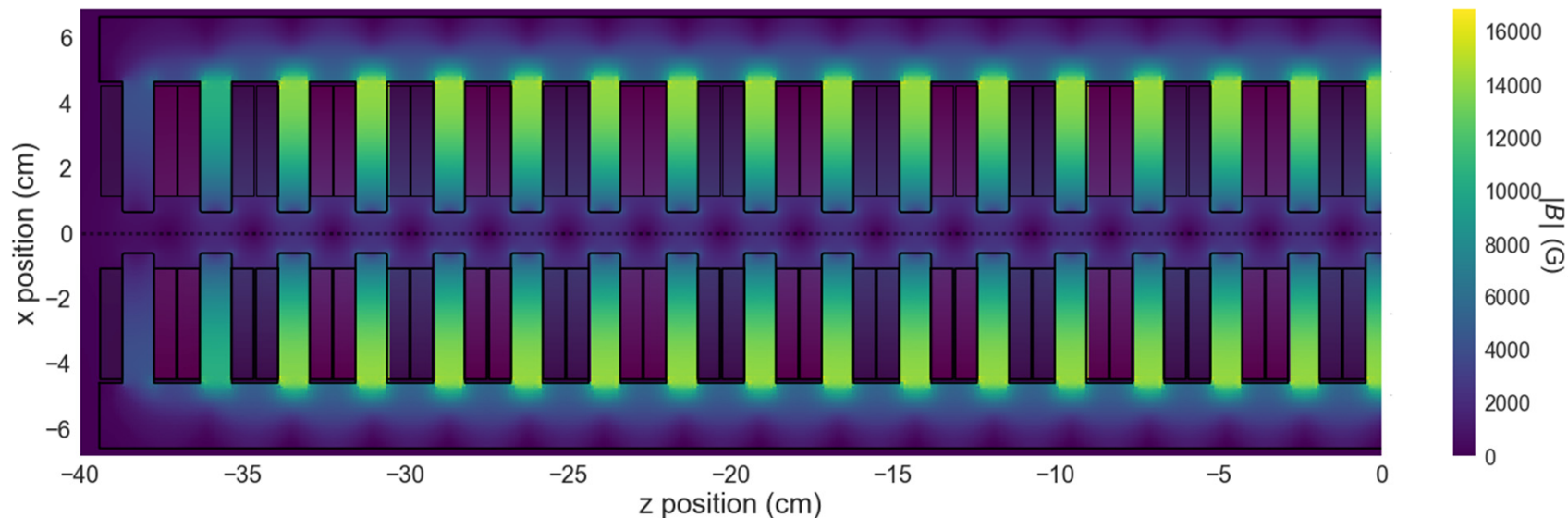


Contamination from IOTA dipole reasonably low



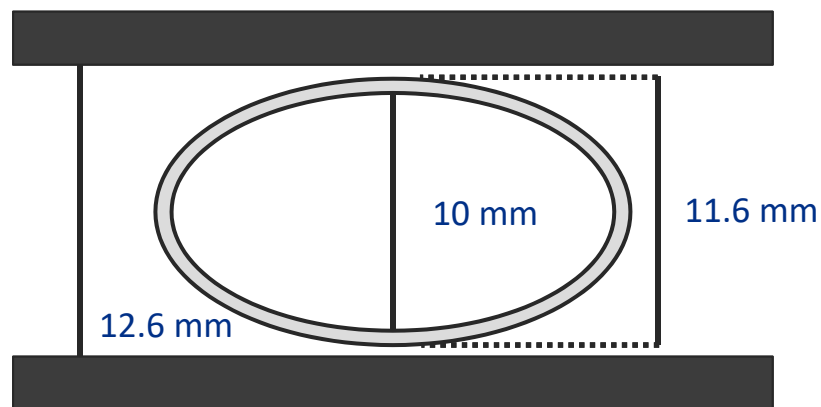
- Radiation from Und. and Dipole not well separated in time (~100 fs)
- ~85% of photons in the fundamental band will be from the undulator
- With aperture on output window: >90%

1- μm undulator design is underway



Current Undulator Design

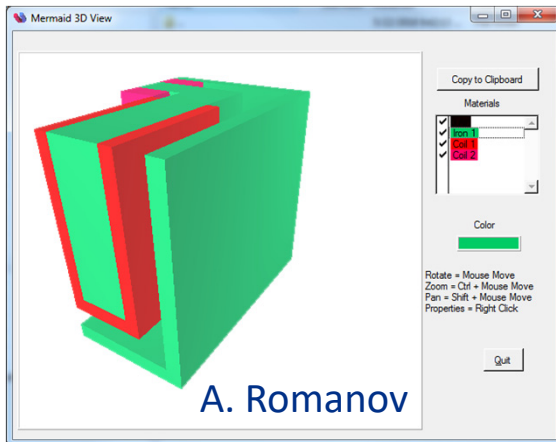
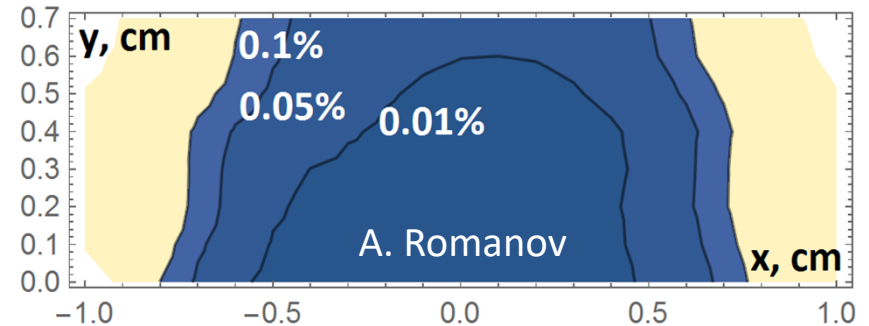
- EM undulator: [1/4,3/4] terminations
- 12.6-mm gap; 0.5-mm clearance
- Elliptical chamber: 0.8-mm walls, 10-mm vertical (inside) and \sim 25-mm horizontal
- Coils: \sim 6x34mm, \sim 6 A/mm², 25.6 A & \sim 61 V
- With AWG12, square Cu ($f\sim$ 0.91): 58 turns, \sim 54 Watts/coil, 1.57 kW per side
- Indirect cooling w/yoke & interstitial fins



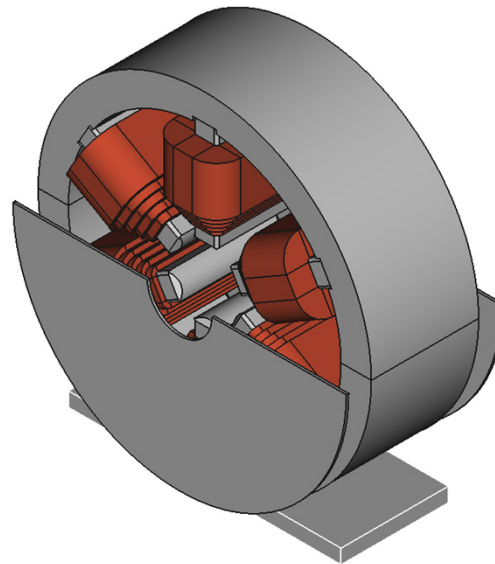
Design/Eng. of dipoles and sextupoles completed

- Monolithic dipole core to maximize field quality
- Shortened version of IOTA sextupole for bypass
- Panofsky quad for coupling horizontal and longitudinal DOF; doubles as vertical corrector

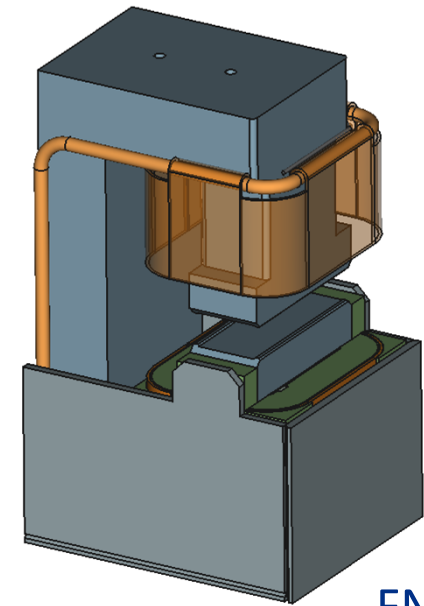
Integrated field quality



Panofsky quad/corrector



Modified IOTA sextupoles



FNAL TD

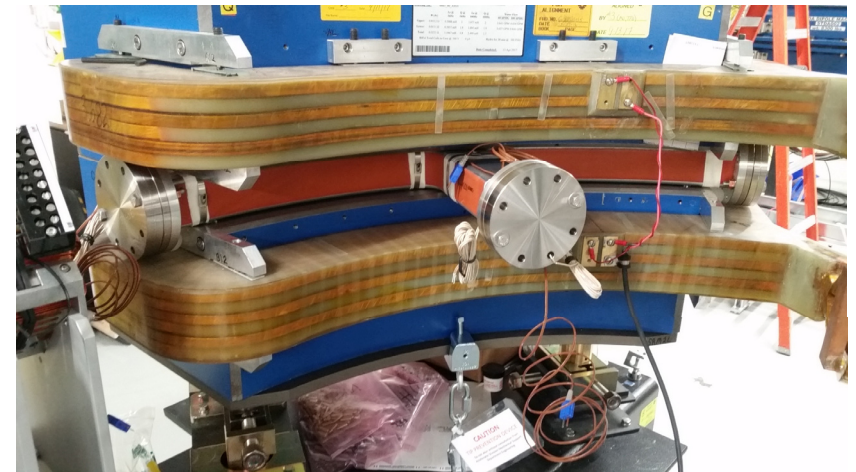
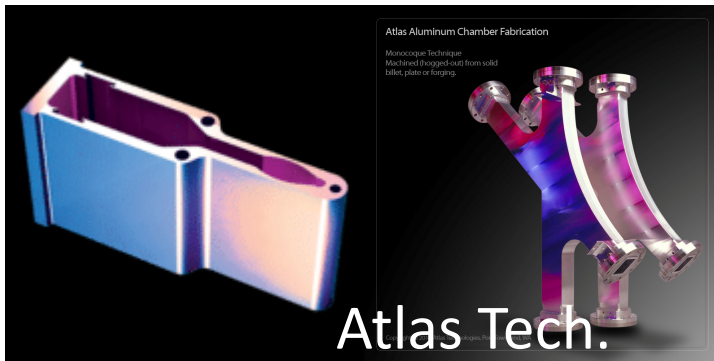
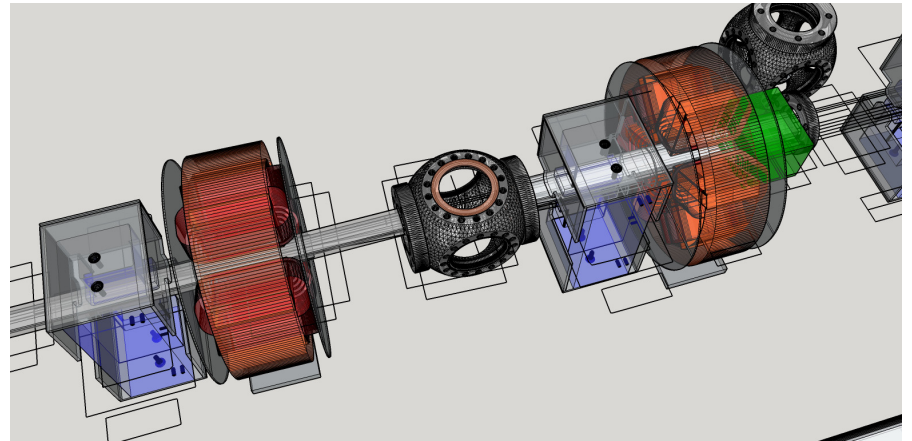
Integrated commercial motion solutions to reduce risk

- Smarpod from SmarAct; hexapod like with 0.5-kg normal load, 0.25-kg trans.
- Provides full 6-DOF motion with sufficient throw; non-mag. & good to $\sim 10^{-11}$ Torr; bakeable up to ~ 130 °C
- SmarAct rotary stages for precision delay/shift stage, same load, mag., vac. and baking performance



Solid models being built for $1\mu\text{m}$ & $2\mu\text{m}$

- Systems integration, chamber design and collision avoidance
- Considering seam-welded construction with 316LN; determining acceptable level of permeability in the welds
- If field errors too large, can use extruded or seam-welded UHV aluminum chambers; similar to IOTA main dipole chambers



FAST injector successfully commissioned at up to 300MeV

- Injector and high-energy beamline are fully operational and ready for OSC program.
- Ongoing upgrades to FAST drive laser infrastructure will expand possibilities for active OSC program at $2\ \mu\text{m}$



IOTA construction is progressing and on schedule

- Expect opportunity for OSC-insertion installation in mid'19
- Additional experiments on the high-energy beamline after OSC demo in IOTA
- IOTA availability for second OSC run depends on schedule for protons



Thank you to all of our collaborators and colleagues

- OSC team: Matt Andorf, Valeri Lebedev, Henryk Piekarczyk, Philippe Piot, Aleksandr Romanov, Jinhao Ruan
- Swapan Chattopadhyay, Sergei Nagaitsev, Alexander Valishev

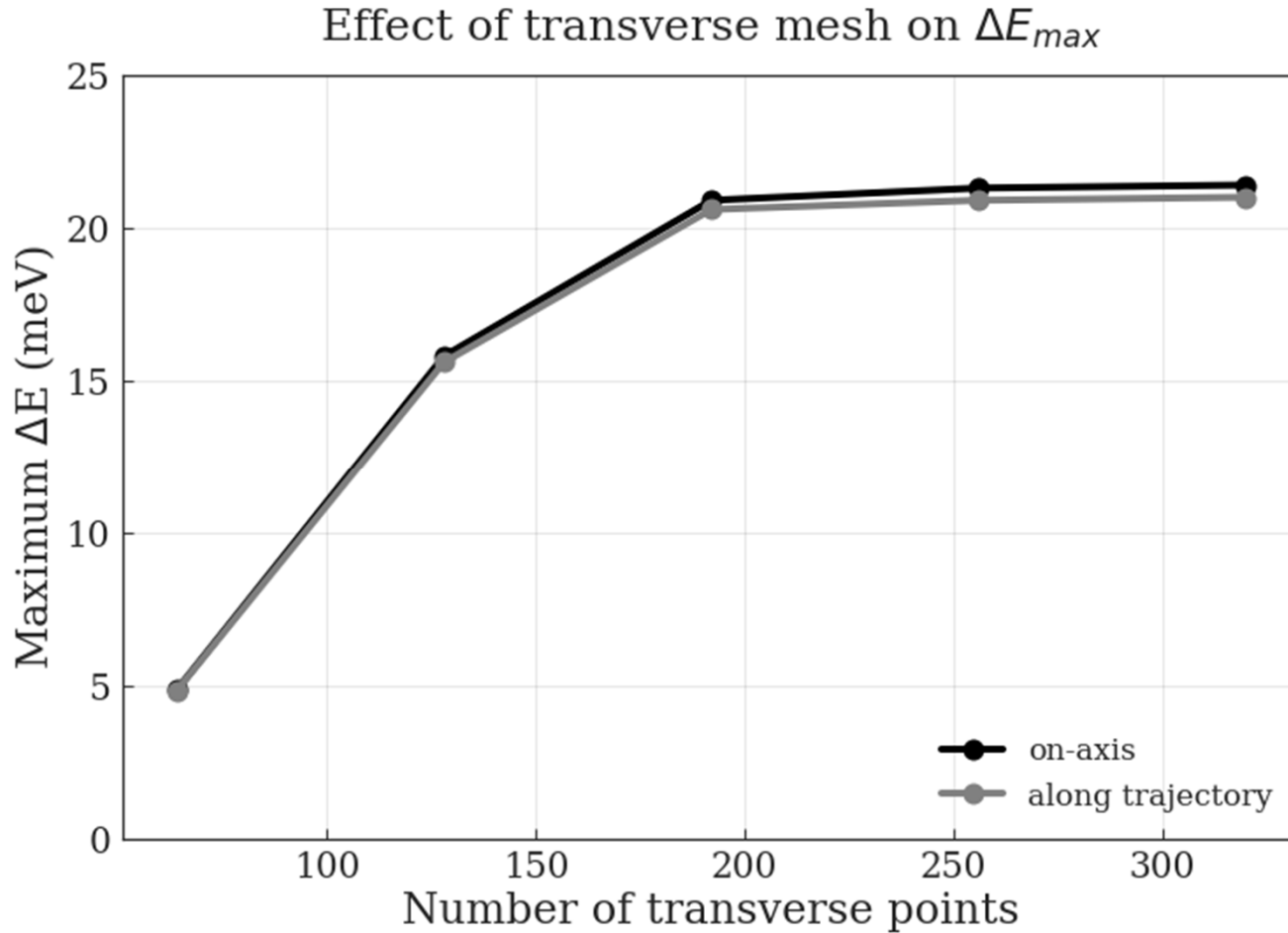
<http://fast.fnal.gov/>

...and thank you for your attention

Fermi National Accelerator Laboratory is operated by Fermi Research Alliance, LLC under Contract No. DE-AC02-07CH11359 with the United States Department of Energy.

EXTRAS

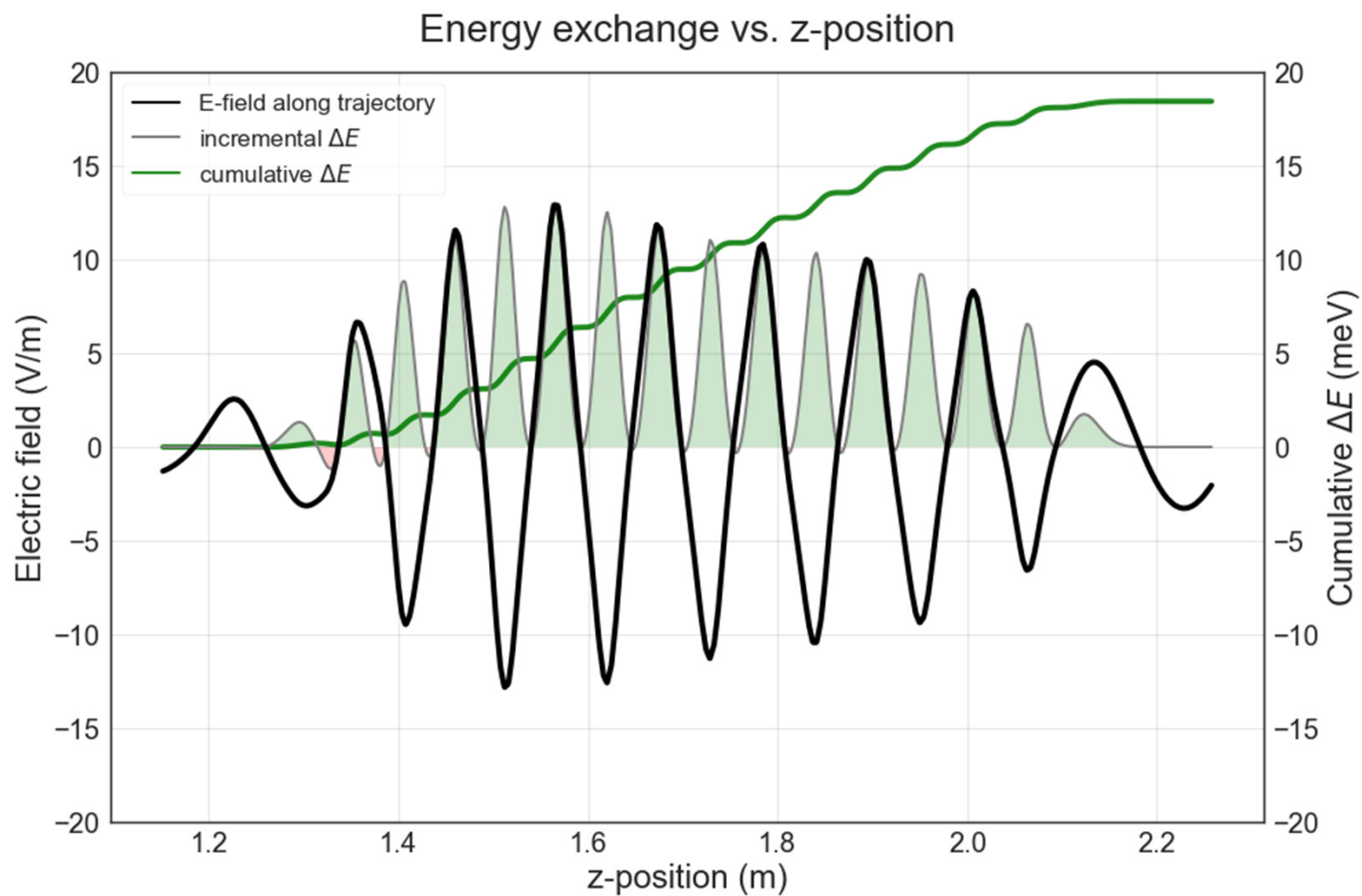
Simulations well converged for $N_x/N_y > 200$



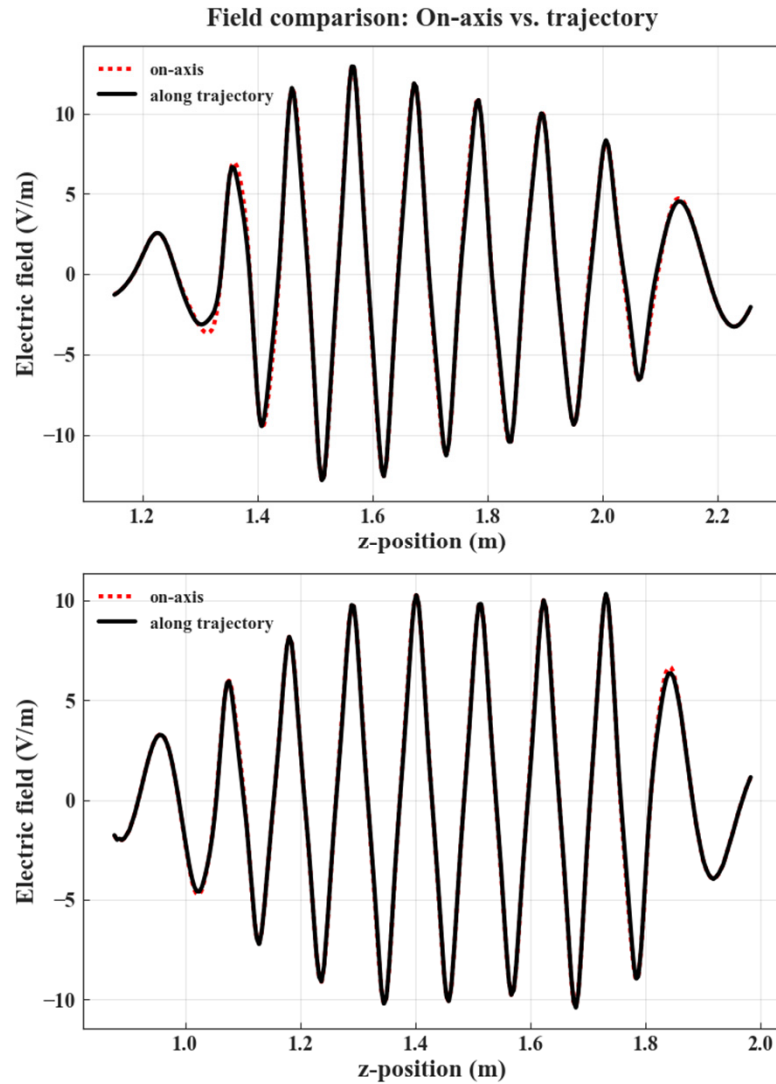
Helpful numbers cheat sheet:

- Ring freq./period: 7.5 MHz/133 ns
- Beam length/duration: ~ 10 cm = 3.3×10^{-10} sec
- Effective duty factor of ring (single bucket; 4 max): 0.25%
- Threshold for BPM use: 50 pC (3.1×10^8 electrons)
- Number of particles in OSC: $\sim 1 \times 10^5$ (15 fC)
- Fund. photon energy: ~ 0.57 eV (2nd: ~ 1.13 eV; 3rd: ~ 1.7 eV)
- Avg. radiated energy/particle/turn/undulator: ~ 31 meV ($\gamma\theta=0.8$)
- Avg. radiated energy; only harmonic content: ~ 20 meV ($\gamma\theta=0.8$)
- Avg./peak harmonic power (1×10^5 electrons): 2.4 nW/ $10 \mu\text{W}$

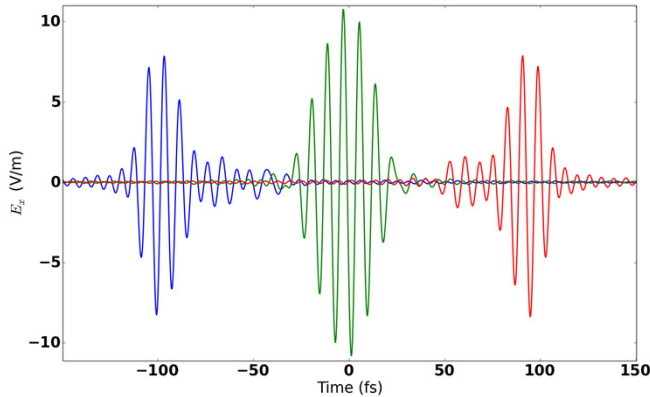
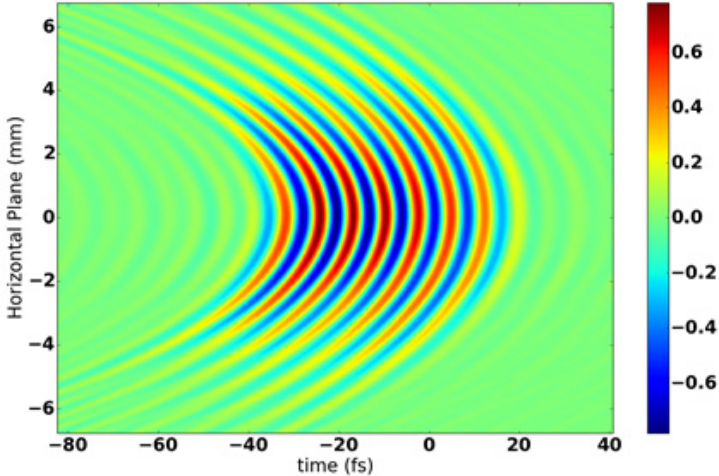
Energy exchange plot



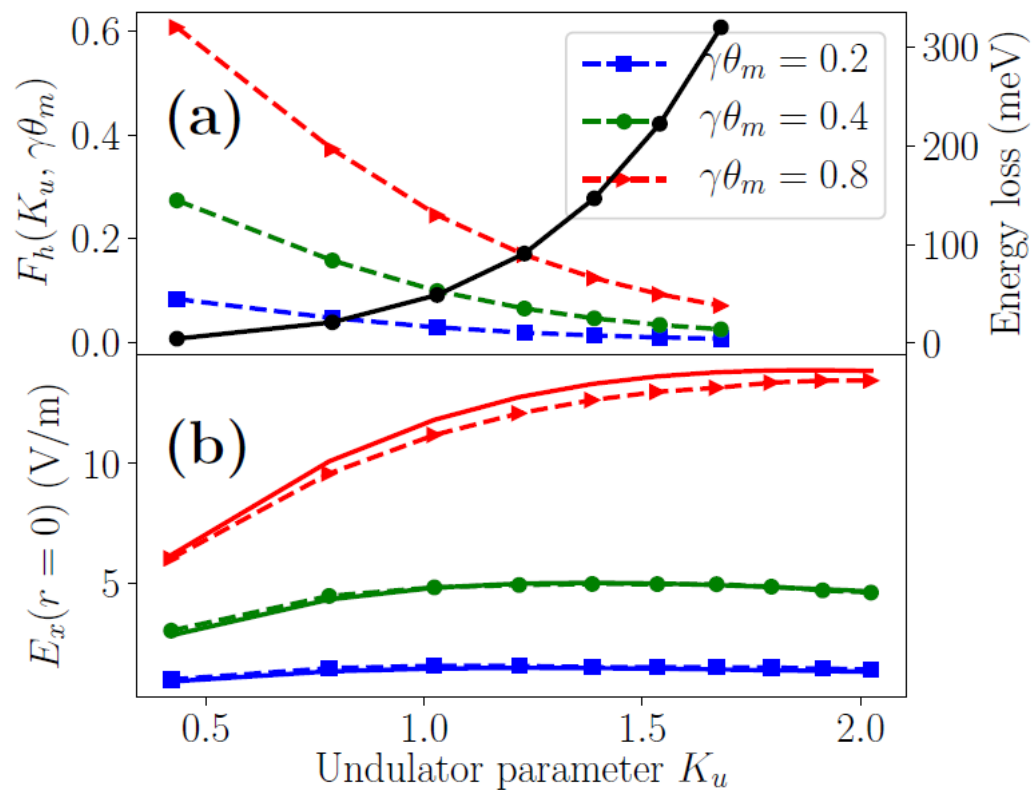
Fields for single lens and telescope (2 μm)



Time-domain structure of wavefront

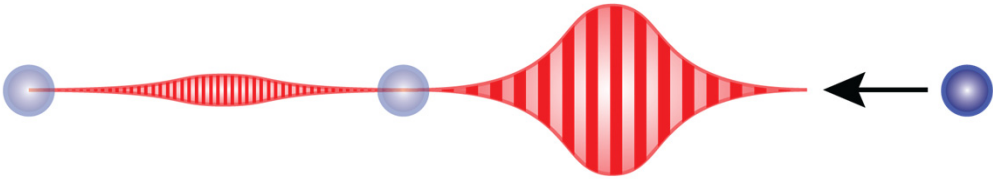


Correction factor for large K



(M. Andorf)

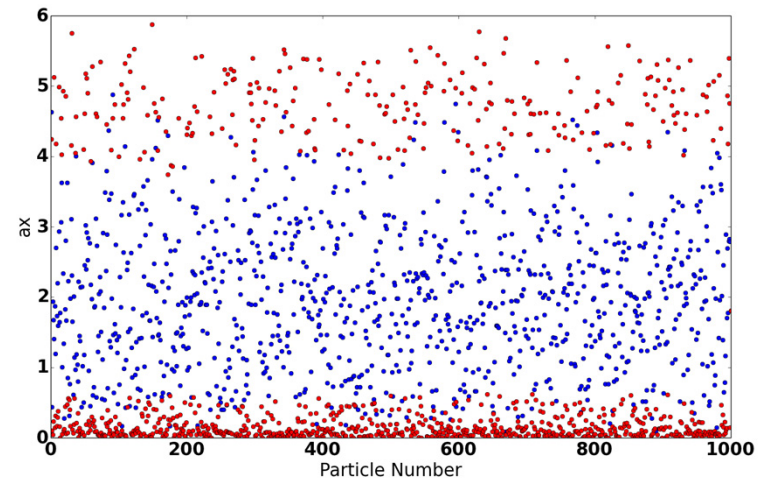
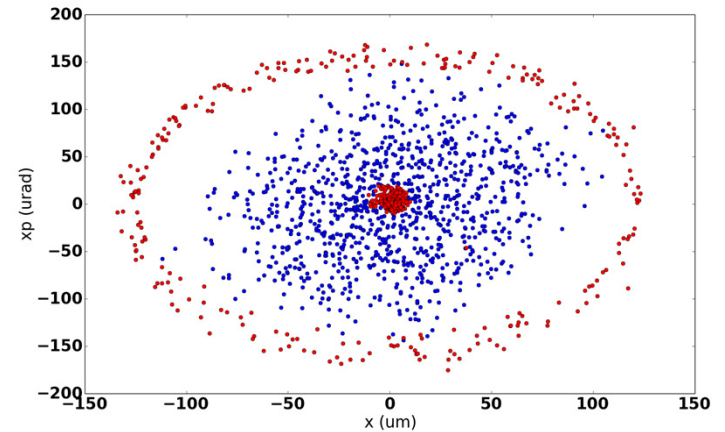
Slippage



$$\delta t = \frac{z (1 - \bar{\beta}) + \frac{K_u^2}{8\gamma^2 k_u} \sin(2k_u z)}{c}$$

Particles will accumulate in damping zones on this surface

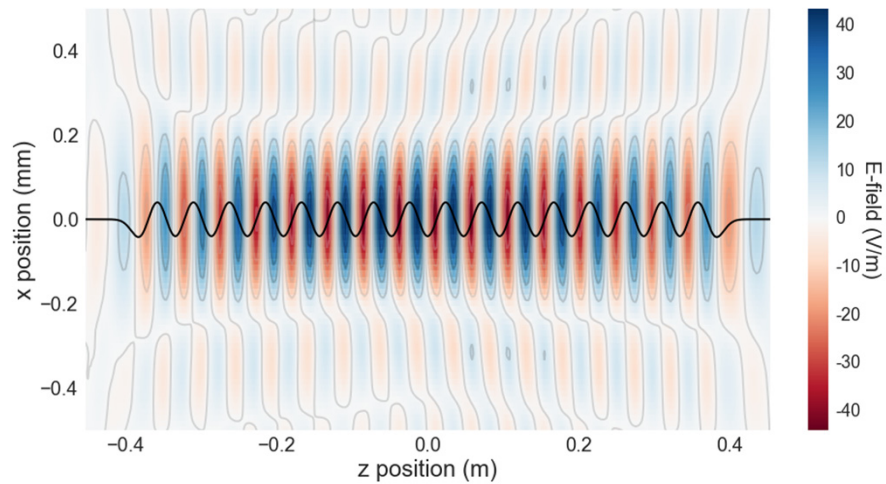
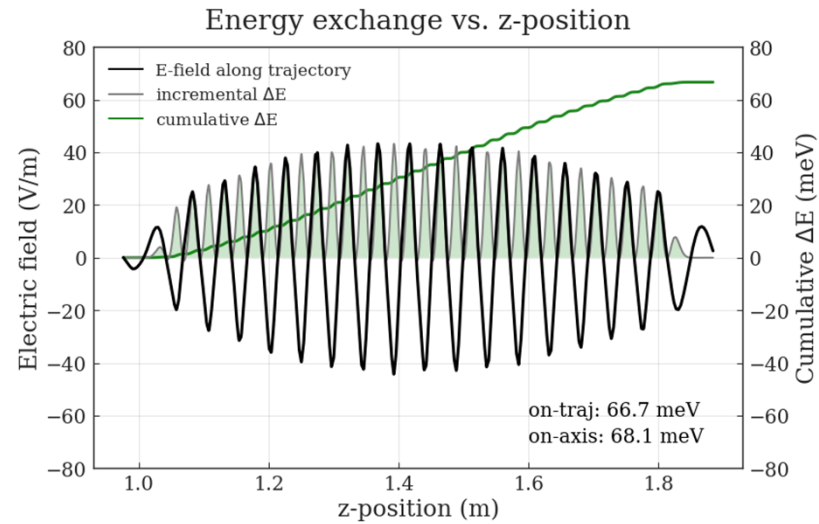
- e.g. preliminary simulations in ELEGANT where wavelength has been reduced to $\sim 400\text{nm}$ to exaggerate the effect
- Shorter wavelength reduces cooling range, allowing beam to sample more of the cooling space.
- Large gain was used to reduce run time
- Such phase space structure might be observable in our experiments



(M. Andorf)

See also: A. Zholents, Phys. Rev. ST Accel. Beams, 15, 032801 (2012)

Hypothetical telescope at 1 μm



Most critical OSC parameters: cooling rates and ranges

- In the linear approximation, path lengthening is:

$$s = M_{51}x + M_{52}x' + \left(M_{56} - \frac{L_{pk}}{\gamma^2} \right) \frac{\Delta p}{p}$$

$$x = x_{\beta} + D \frac{\Delta p}{p},$$

$$x' = x'_{\beta} + D' \frac{\Delta p}{p}$$

- In absence of betatron oscillations:

$$s = \left(M_{51}D + M_{52}D' + M_{56} - \frac{L_{pk}}{\gamma^2} \right) \frac{\Delta p}{p} = S_{pk} \frac{\Delta p}{p}$$

- Can estimate cooling rate (1/s) for longitudinal emittance as:

$$\lambda_s = f_0 \kappa k_0 S_{pk}$$

M_{56} and S_{pk} must be different to have horizontal cooling

- Sum of friction decrements then sets value of horizontal cooling

$$\lambda_x = f_0 \kappa k_0 \left(M_{56} - S_{pk} - \frac{L_{pk}}{\gamma^2} \right)$$

- So for a given setting of the chicane (M_{56}) the cooling ratio is determined by the dispersion and its derivative at the exit of the pickup.

$$s = \left(M_{51}D + M_{52}D' + M_{56} - \frac{L_{pk}}{\gamma^2} \right) \frac{\Delta p}{p} = S_{pk} \frac{\Delta p}{p}$$

- We can then couple the horizontal and vertical DOF elsewhere in the ring to achieve full 6D cooling.

$$\frac{\lambda_x}{\lambda_s} = \frac{M_{56}}{S_{pk}} - 1$$

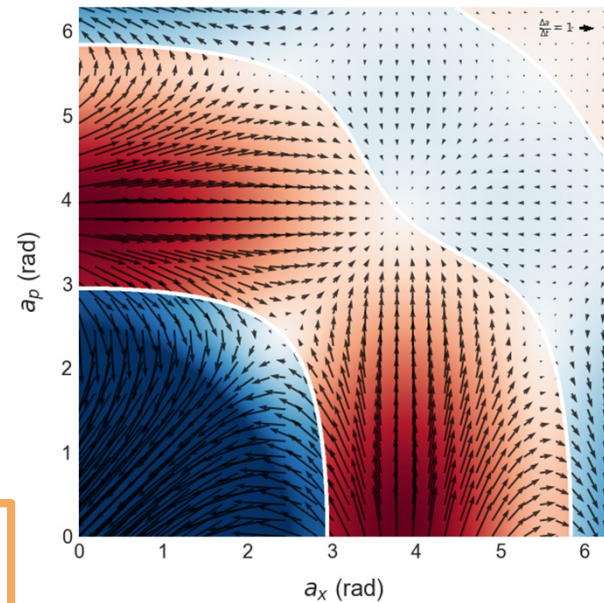
OSC creates a cooling/heating surface in phase space

- On successive passes through the cooling insertion, particles will have different betatron and synchrotron coordinates
- Path lengthening depends on these coordinates, and the cooling force on a given pass increases or decreases
- This creates a cooling/heating surface that particles will move along
- Integrating over betatron and synchrotron periods reveals the cooling range for OSC:

$$\frac{\delta p}{p} = -\kappa \sin(a_x \sin \psi_x + a_p \sin \psi_p)$$

$$a_p = -k_0(M_{51}D + M_{52}D' + M_{56}) \left(\frac{\Delta p}{p} \right)_m$$

$$a_x = -k_0 \sqrt{\tilde{\varepsilon}(\beta M_{51}^2 - 2\alpha M_{51}M_{52} + (1 + \alpha^2)M_{52}^2/\beta)}$$



$$\mu_{01} = 2.405$$

$$\begin{bmatrix} F_x \\ F_s \end{bmatrix} = \begin{bmatrix} \lambda_x(a_x, a_p)/\lambda_x \\ \lambda_s(a_x, a_p)/\lambda_s \end{bmatrix} = 2 \cos(k_0 s_0) \begin{bmatrix} J_0(a_p)J_1(a_x)/a_x \\ J_0(a_x)J_1(a_p)/a_p \end{bmatrix}$$

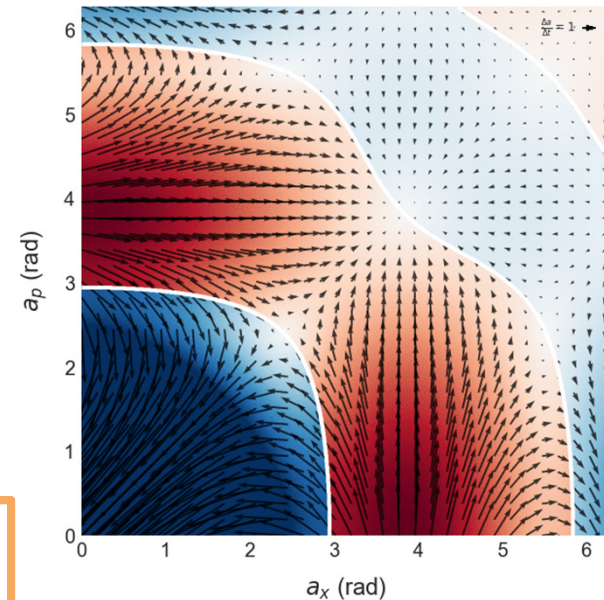
OSC creates a cooling/heating surface in phase space

- On successive passes through the cooling insertion, particles will have different betatron and synchrotron coordinates
- Path lengthening depends on these coordinates, and the cooling force on a given pass increases or decreases
- This creates a cooling/heating surface that particles will move along
- Integrating over betatron and synchrotron periods reveals the cooling range for OSC:

$$\frac{\delta p}{p} = -\kappa \sin(a_x \sin \psi_x + a_p \sin \psi_p)$$

$$a_p = -k_0(M_{51}D + M_{52}D' + M_{56}) \left(\frac{\Delta p}{p} \right)_m$$

$$a_x = -k_0 \sqrt{\tilde{\varepsilon}(\beta M_{51}^2 - 2\alpha M_{51}M_{52} + (1 + \alpha^2)M_{52}^2/\beta)}$$



$$\mu_{01} = 2.405$$

$$\begin{bmatrix} F_x \\ F_s \end{bmatrix} = \begin{bmatrix} \lambda_x(a_x, a_p)/\lambda_x \\ \lambda_s(a_x, a_p)/\lambda_s \end{bmatrix} = 2 \cos(k_0 s_0) \begin{bmatrix} J_0(a_p)J_1(a_x)/a_x \\ J_0(a_x)J_1(a_p)/a_p \end{bmatrix}$$

Cooling ranges depend on delay and wavelength

$$\varepsilon_{max} = \frac{\mu_{01}^2}{k_0^2(\beta M_{51}^2 - 2\alpha M_{51}M_{52} + (1 + \alpha^2)M_{52}^2/\beta)}$$

$$n_{\sigma x} = \sqrt{\frac{\varepsilon_{max}}{\varepsilon}}$$

$$\left(\frac{\Delta p}{p}\right)_{max} = \frac{\mu_{01}}{k_0 S_{pk}}$$

$$n_{\sigma p} = \frac{\left(\frac{\Delta p}{p}\right)_{max}}{\sigma_p}$$

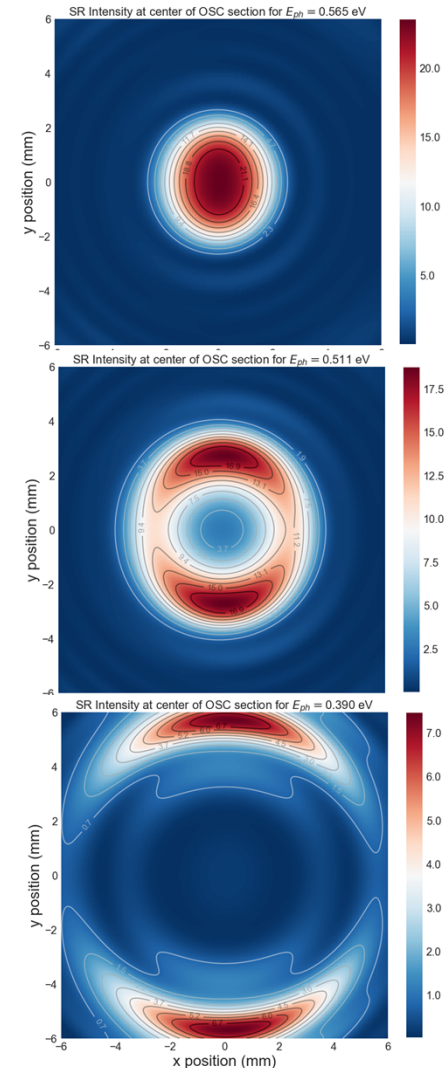
- Designing an effective OSC system means setting a balance between cooling ranges and rates

Simulations performed with Sync. Rad. Workshop

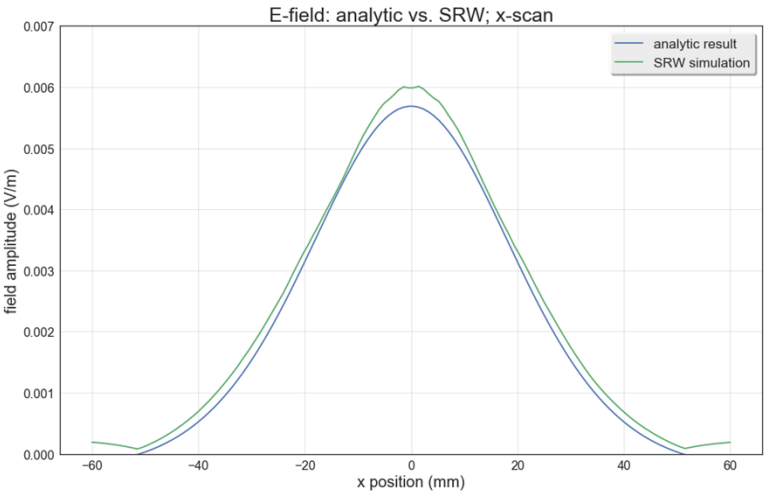
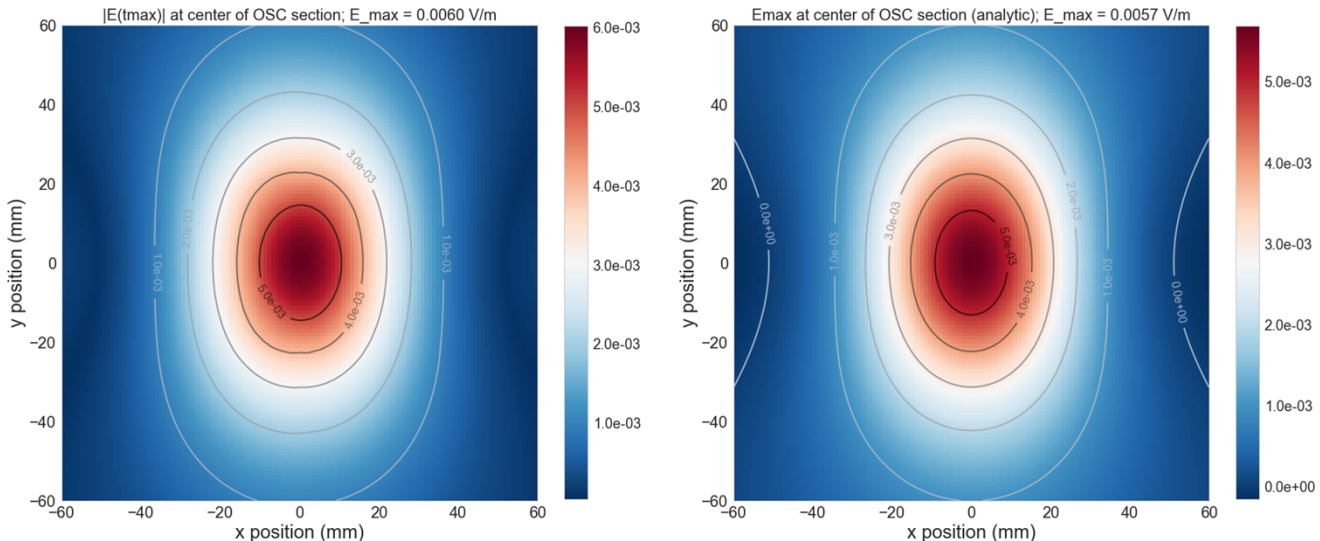
Wave-optics simulation code. Developed in 1990's, primarily for the simulation of beamlines at light sources.

- 1) Radiation wavefront is generated by particle traversing specified mag. Field
- 2) Wavefront is propagated through optical system in the spectral domain.
- 3) Fields are converted into time domain.
- 4) Compute slippage and determine field experienced by the co-propagating particle (particle does not modify wavefront in KU)

O. Chubar, P. Elleaume, Proc. EPAC98, Stockholm Sweden, p.1177 (1998).

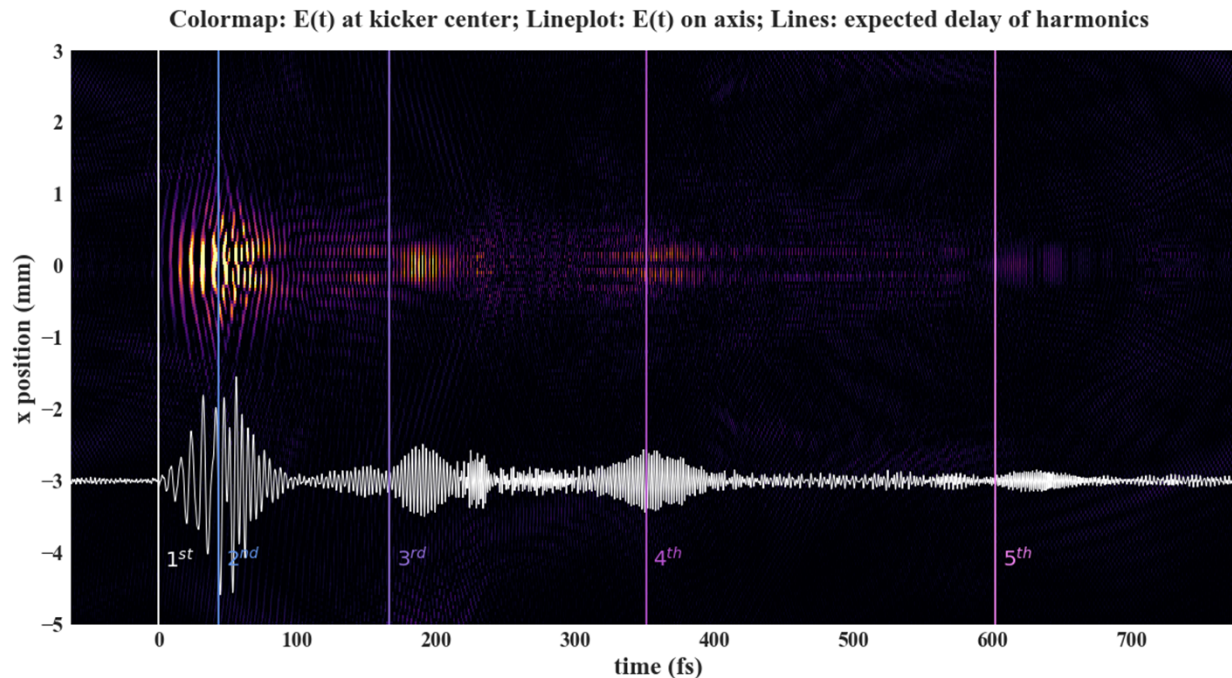


Good agreement with analytic approximations in the appropriate regime ($K \ll 1, R \gg L_{und}$)



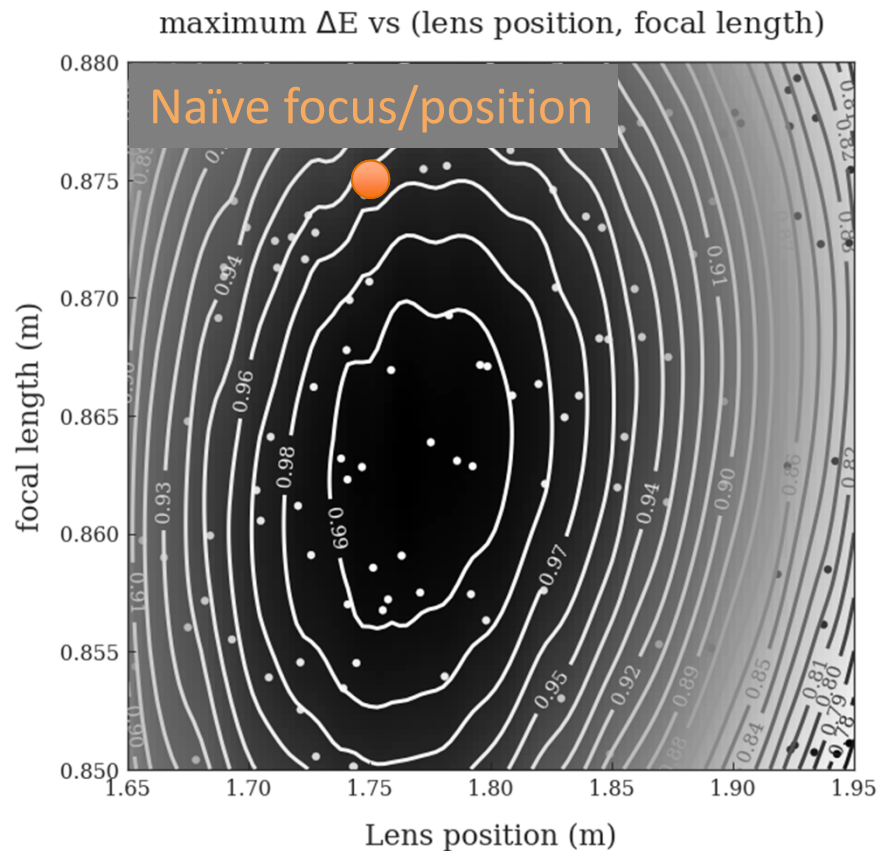
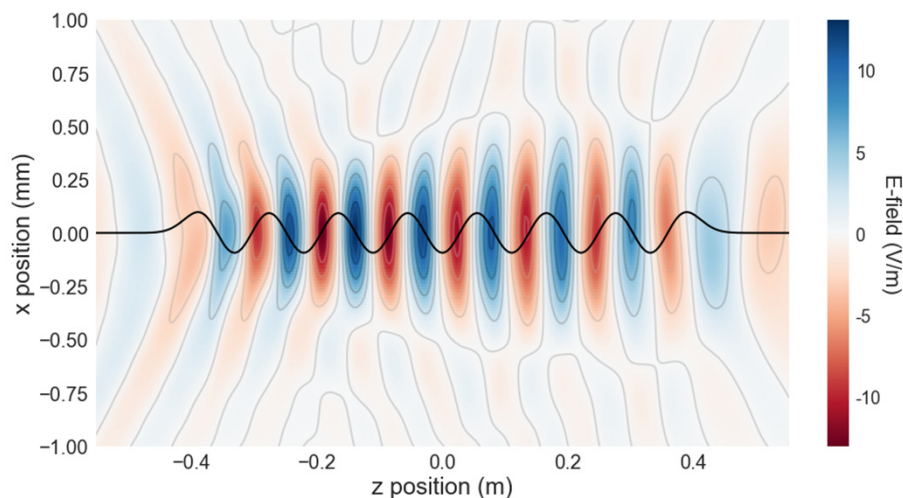
Custom routines for dispersive optics

- Index of refraction described w/ the Sellmeier equation
- Custom optics routines based on SRW's transmission element
- Captures “all” orders of dispersion
- Observe appropriate delays and broadening



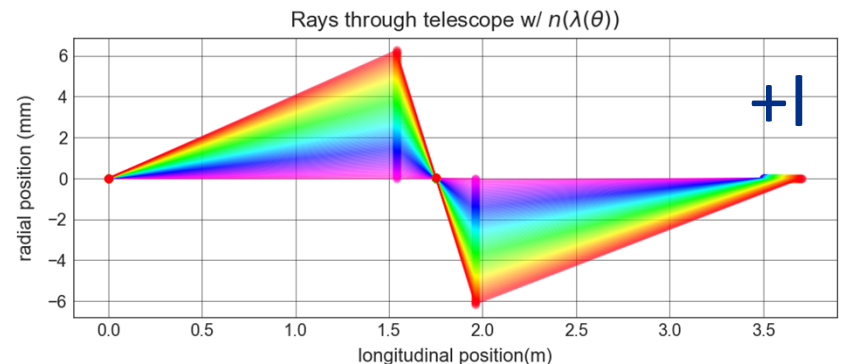
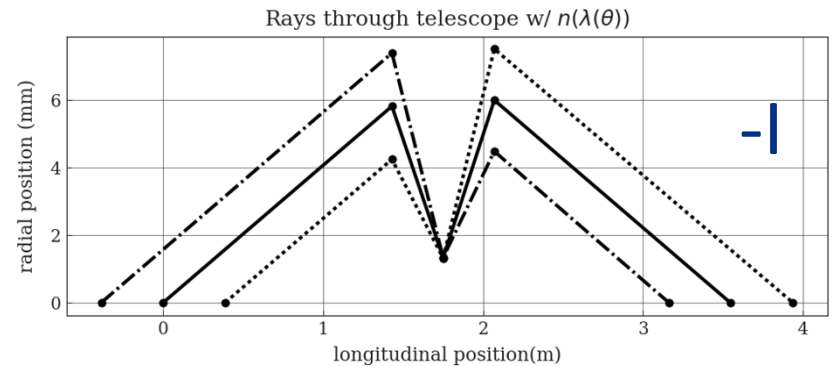
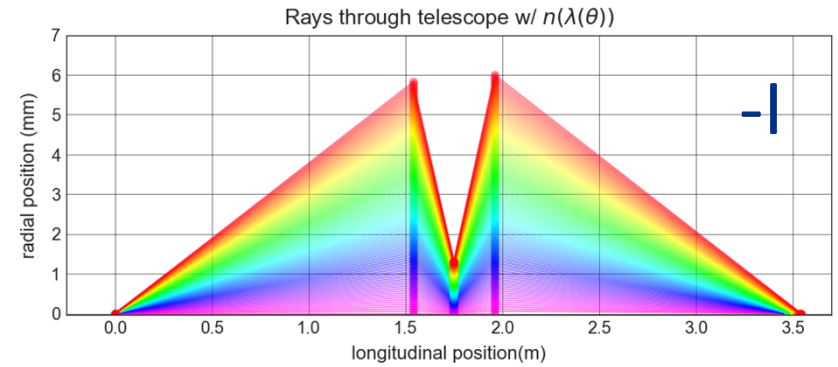
Optimal lens strength and position from SRW sims

- Key parameter to optimize is maximum energy exchange.
- For single lens case, an increase of $\sim 5\%$ is possible due to over focusing and smaller ratio of und. length to lens distance

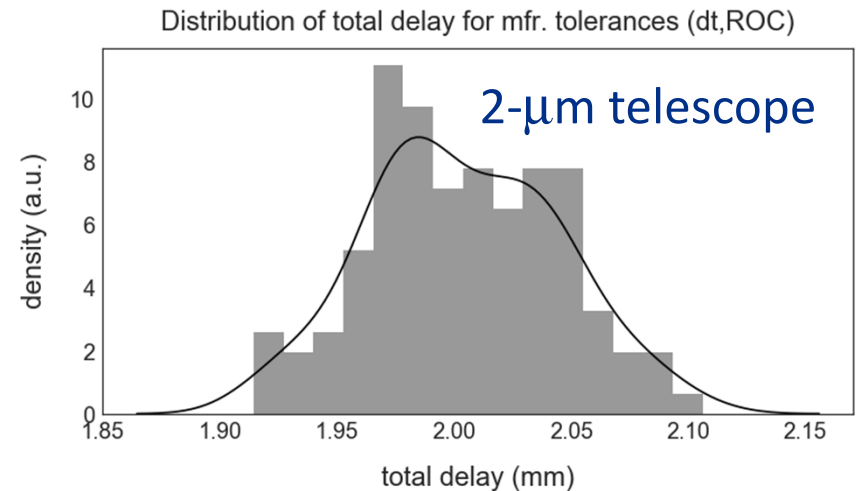
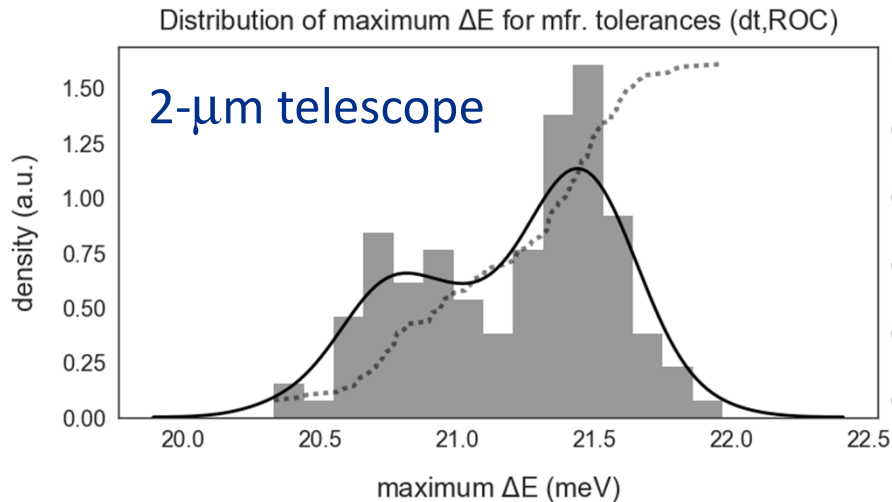


Two telescopic configurations are considered

- Two telescope configurations with different mappings: +I and -I
- -I tele. suppresses depth of field and more closely matches the horizontal mapping of the beam bypass
- +I tele. more closely matches the vertical mapping of the beam bypass
- Mismatch between optics and beam mapping can actually increase cooling range by field reduction in antidamping zones



Optics manufacturing spreads acceptable (BaF₂)

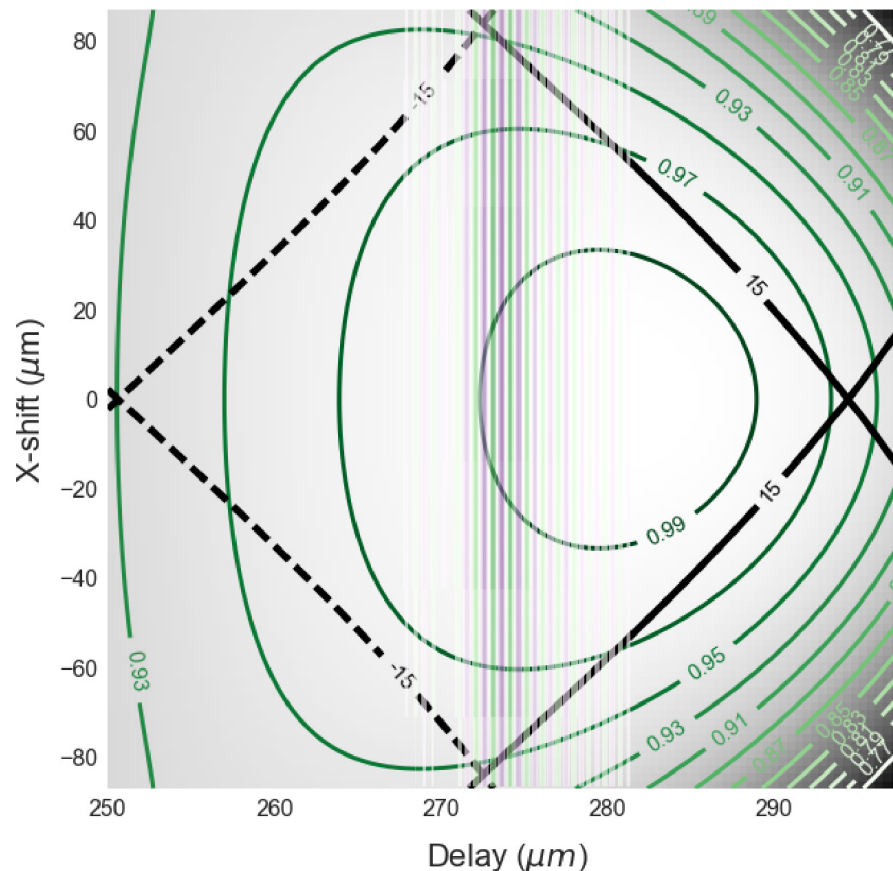


- Monte Carlo simulations using central thickness and ROC spreads from manufacturer
- ~5% spread in maximum kick value
- Tolerances are primarily set by manufacturing dropout, so to a point, can get higher tolerance for somewhat higher price
- Deviations in central thickness of lenses could be measured and applied to fabrication of delay plates

Delay surface overlaid with radiation profile

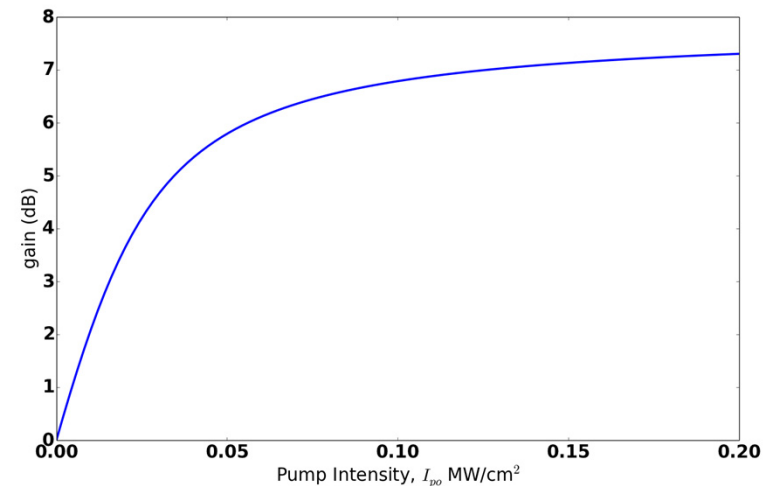
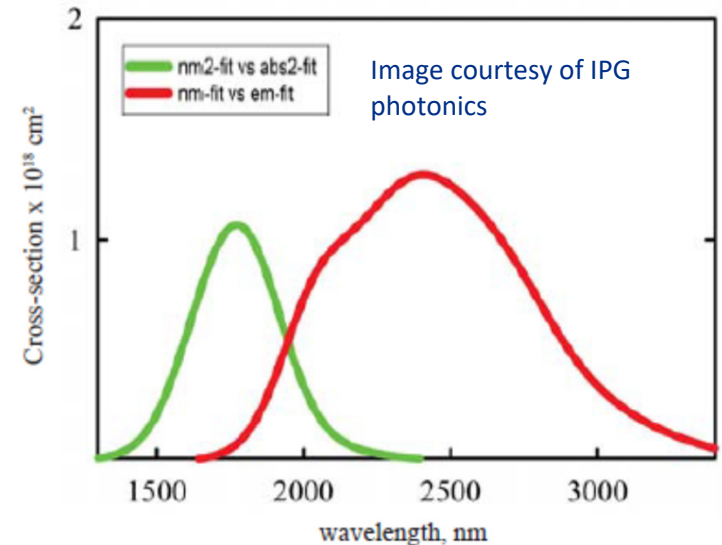
- For reference, 230 steps at 3 m° (0.69°) each is $\sim 1 \mu\text{m}$
- Can traverse this angular range in $\sim 10 \text{ ms}$
- Steps can go as low as 0.3 m°

Transmittance vs $(\Delta s, \Delta x)$: $t=250\text{-}\mu\text{m}$, $\lambda = 0.95\mu\text{m}$; $\theta_B = 7^\circ$



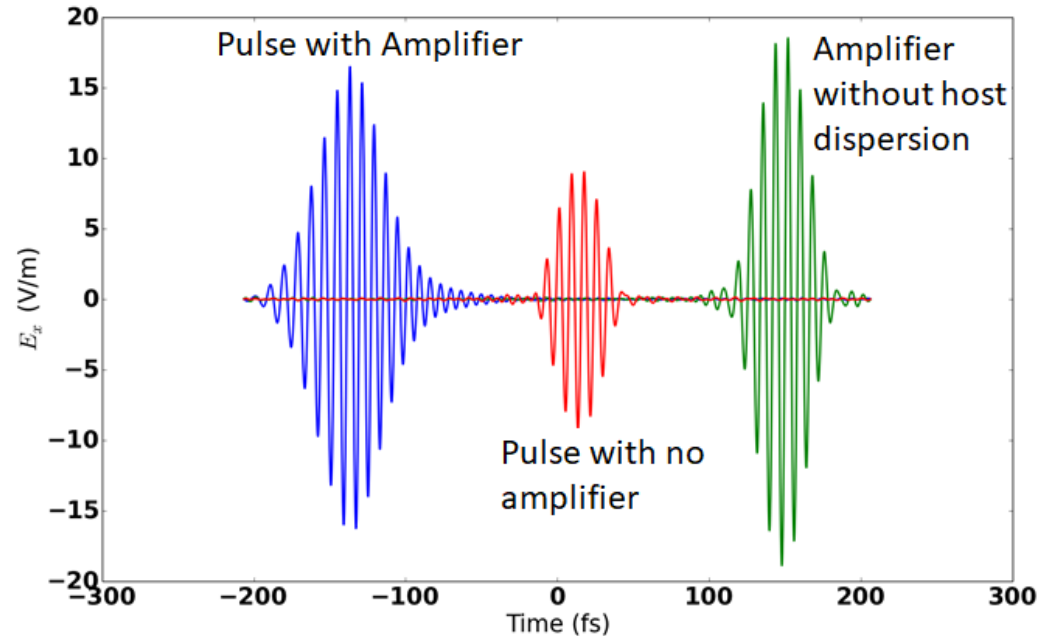
For 2 μm , a low-gain Cr:ZnSe amplifier is possible

- Amplifier requires focusing inside of telescope, so positive identity must be used
- Cr:ZnSe crystal
 - Center wavelength 2490 nm
 - 50 THz bandwidth
 - 1-mm crystal length (optical delay of 1.43 mm)
 - single pass gain 7dB
 - Saturable absorption major limiter in gain
- Pumped by a thulium fiber laser
 - Wavelength, 1910 nm
 - 100 W max power
 - Continuous Wave (CW) operation but capable of 1 kHz frequency modulation (mitigates thermal effects).

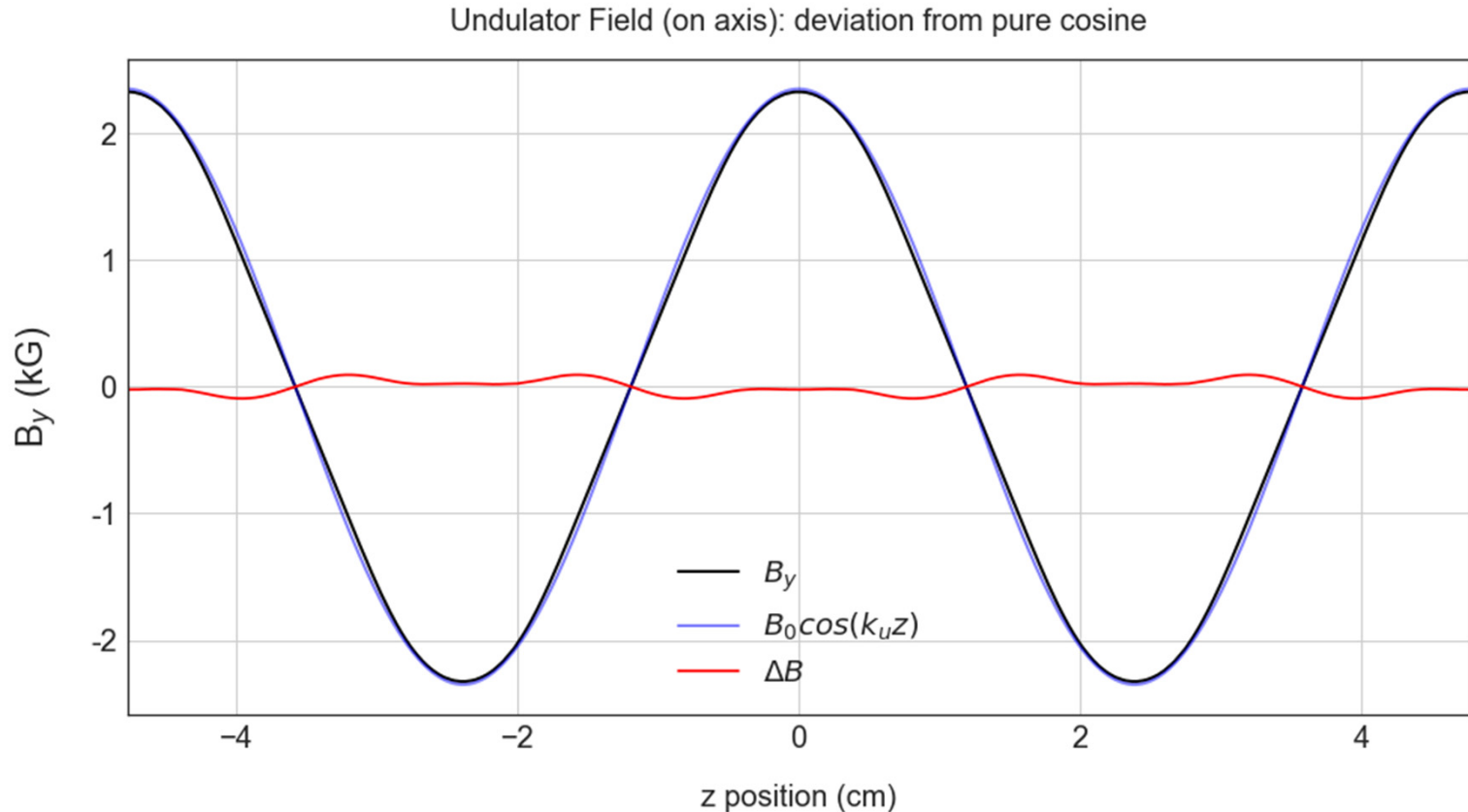


Amplifier routine to estimate performance in SRW

- Predicted 7dB power gain (2.24x in field) for plane wave at emission peak
- Actual amplification of packet reduced by:
 - Finite bandwidth of amplifier ($\downarrow 14\%$)
 - GVD in crystal ($\downarrow 12\%$)
- Max amplification in SRW: 1.8x in field and energy kick



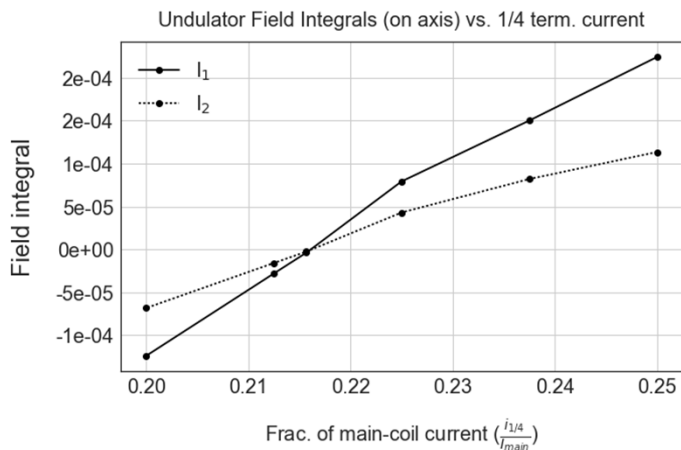
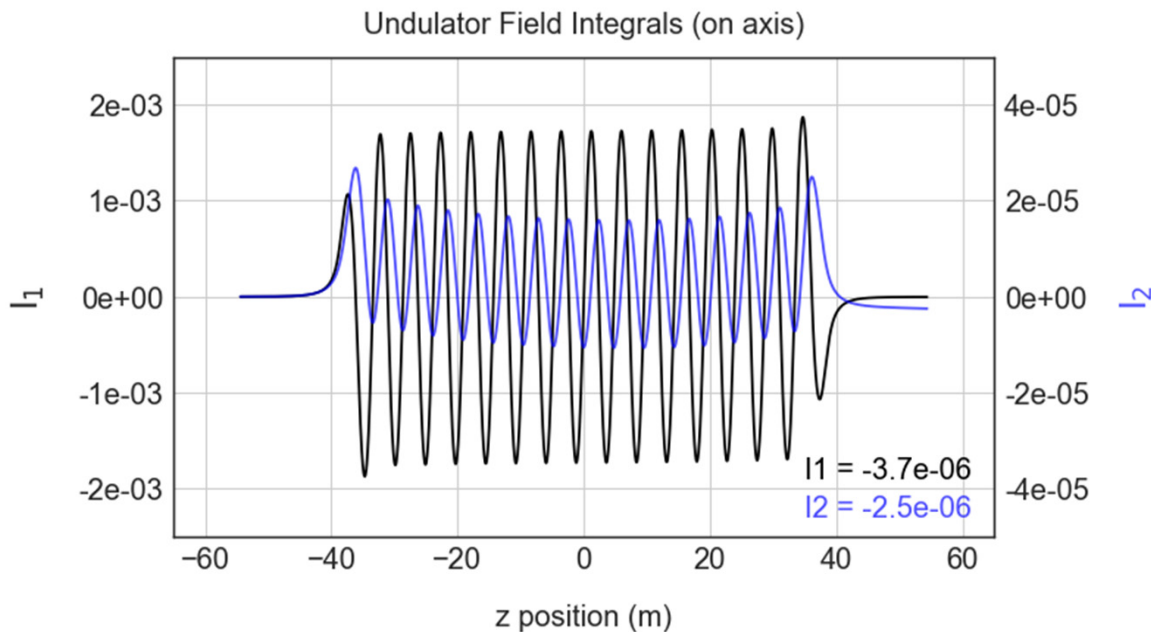
Deviations from a pure cosine are small



- No special optimization performed
- Slight increase in harmonic content; should be irrelevant for OSC

[1/4 , -3/4] terminations to minimize trajectory offset

- Transverse offset and angle of trajectory at exit can be expressed in terms of the field integrals
- Termination-coil currents are tuned to ensure field integrals are near zero
- Full coils with precision, high-power shunt resistors for setting operating current



$$I_{1y} = \int_{z_0}^{z_f} B_y(z) dz \quad x' = -\frac{q_e}{\gamma m_e \beta_z c} I_{1y} \approx 11 \mu\text{rad}$$

$$I_{2y} = \int_{z_0}^{z_f} \int_{z_0}^{z'} B_y(z) dz dz' \quad x = -\frac{q_e}{\gamma m_e \beta_z c} I_{2y} \approx 7 \mu\text{m}$$

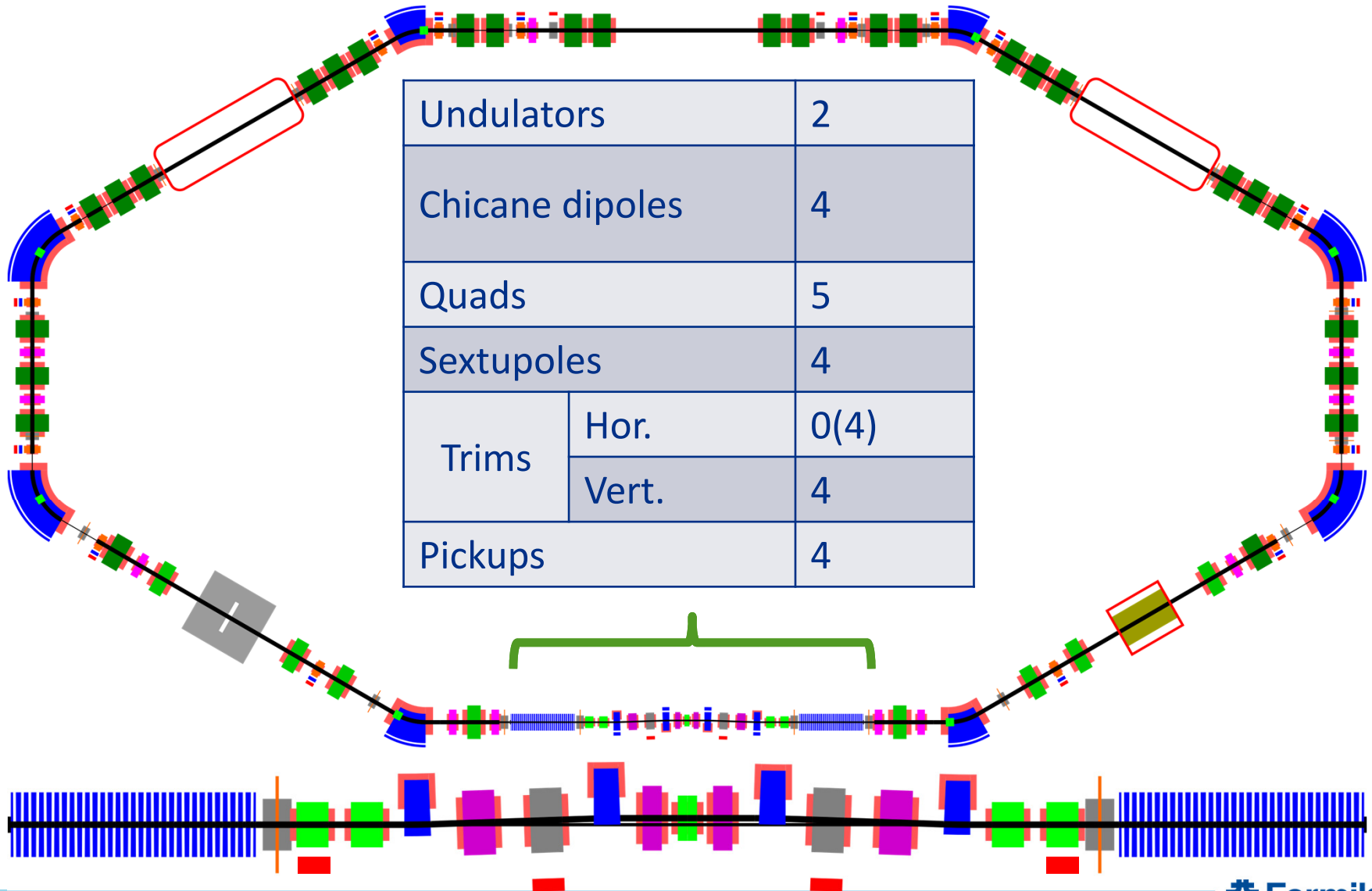
Main parameters of IOTA with OSC

A. Romanov

Momentum	100 MeV	
Circumference	39.97 m	
Vacuum	1×10^{-10} torr	
Number of particles	10^6 e, 5 μ A	
Chicane delay	0.65 mm	2.000 mm
Chicane offset	20.09 mm	35.12 mm
OSC light wavelength	950 nm	2200 nm
Optical instrumentation	Off the shelf	Challenging
Passive cooling	Yes	Yes
Active cooling	No (space)	Yes
RMS emittances at full coupling ($\epsilon_x = \epsilon_y$)	0.5 , nm	1.43 , nm
Betatron tunes (x,y)	(5.41, 2.41)	(5.41, 3.41)

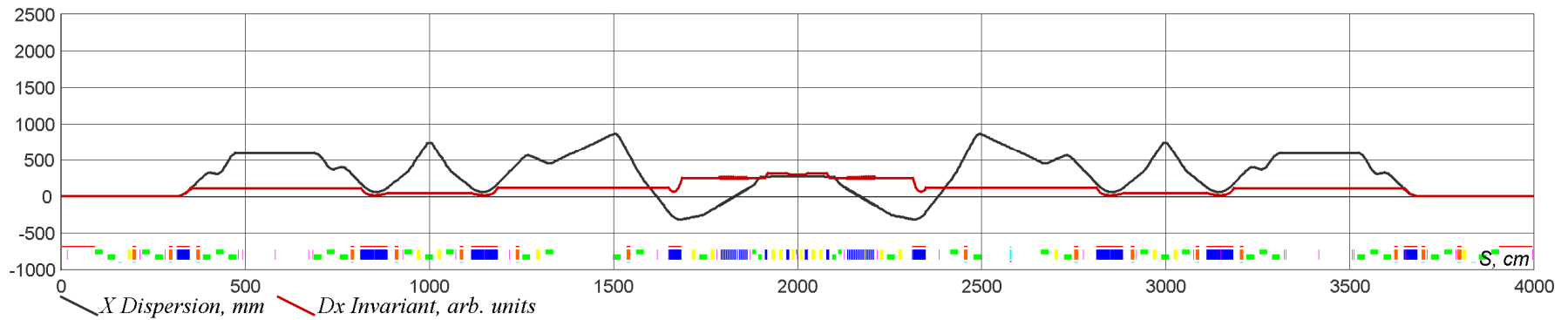
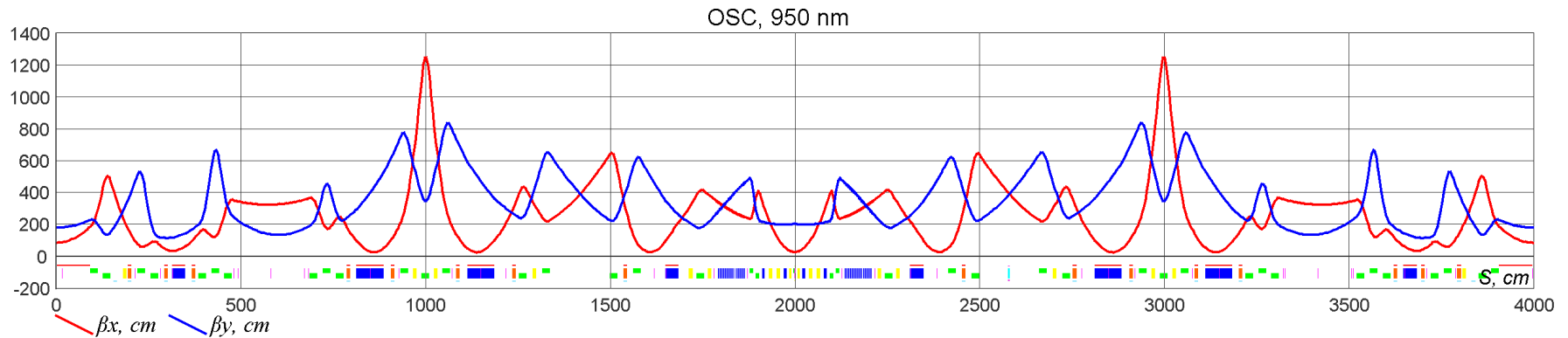
Magnets of OSC insertion

A. Romanov



Linear lattice design for 950 nm

A. Romanov

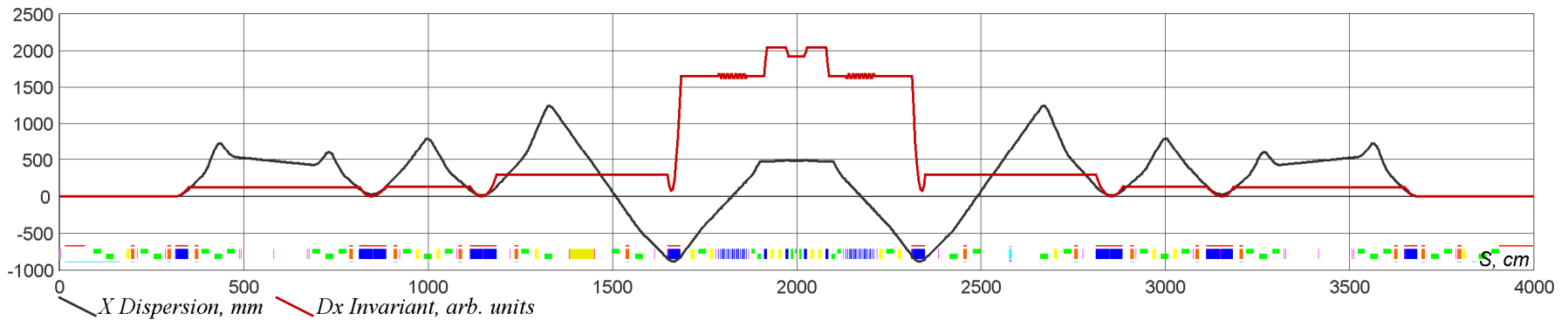
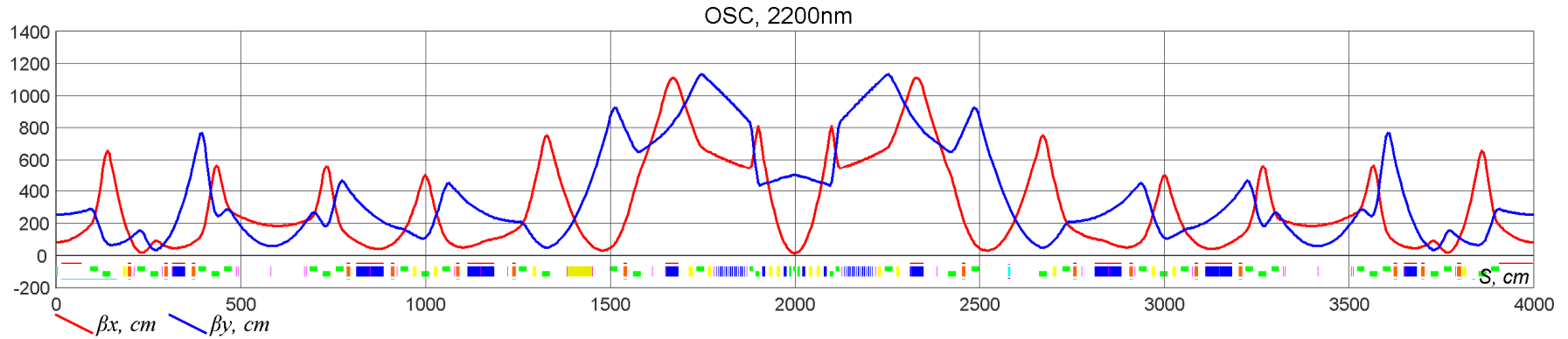


Betas start, x,y	25, 200 cm
D_x start	27 cm
Tunes, x,y	5.42, 2.42
Mom. comp.	0.0025
Emittances, x,y	0.5 E-7 cm

Energy drop	13.4 eV
Bunch length @30V	7.6 cm
Energy spread	1.00 E-4
Sync. Tune @30V	2.05 E-5
Damp. times (x,y,s)	(2.0,2.0,0.985) s

Linear lattice design for 2200 nm

A. Romanov



Betas start, x, y	12, 500 cm
D_x start	48 cm
Tunes, x, y	5.42, 3.42
Mom. comp.	-0.0165
Emittances, x, y	1.44 E-7 cm

Energy drop	13.25 eV
Bunch length @30V	19.9 cm
Energy spread	1.06 E-4
Sync. Tune @30V	5.6 E-5
Damp. times (x, y, s)	(1.9, 1.9, 1.1) s

- Two families of sextupoles are necessary to compensate second order path lengthening, to keep high amplitude electrons in phase with radiation when they receive cooling kick:

$$\Delta s_2 = \frac{1}{2} \int (\theta_x(s)^2 + \theta_y(s)^2) ds$$

- Necessary gradients produce strong nonlinearities and chromaticity that must be corrected
- Regions with small betas are the main contributors to the integral
- For the stability, path lengthening should satisfy:

$$|\Delta s^* k| < 2.4 \text{ rad}$$

Second order path lengthening for 12 sigmas

A. Romanov

- Need of sextupoles for 950nm version is not so obvious

